Table of Contents

1. *General information*

Natural terpenes 1,4-cineole, 1,8-cineole, eucalyptus and turpentine oils were provided by Shanghai Titan Scientific Co., Ltd. Sodium lignosulfonate, 3-mercaptopropyl trimethoxysilane, phenol and guaiacol were supplied by Aladdin Industries. The solid acid sulfate-modified zirconia-titania (SO_4^{2-}/ZrO_2-TiO_2) and phosphotungstic acid modified MCM-41 (HPW/MCM-41) were obtained by Hangzhou Timing Technology Co., Ltd. The solid acid Nafion resin was provided by Jiangsu Success Resin Co., LTD. The solid acid T-62MP resin was obtained from Cohesion (Beijing) Technology Co., Ltd. Molecular sieves including Al-MCM-41, MCM-41, SBA-15, H-Y H-BEA, H-MOR and H-ZSM5 were sourced from Nankai University Catalyst Co., Ltd. Common solvents such as dimethyl carbonate (DMC), dichloroethane (DCE), cyclohexane and hexane were supplied by Xilong Scientific Co., Ltd. All chemicals were of analytical grade and were used as received without further purification. The Pd/C, Pt/C, Ru/C and Rh/C catalysts were provided by Shanghai Titan Technology Co., Ltd. For ease of comparison, the metal content of these catalysts was selected as 5% by weight.

NMR spectra were acquired at room temperature using a 600 MHz spectrometer with $CDCl_3$ as the solvent. Chemical shifts for ^1H NMR are reported in ppm relative to the residual $CHCl_3$ signal (7.26 ppm) as an internal reference. Similarly, ^{13}C NMR chemical shifts are referenced to the central peak of $CDCl_3$ (77.16 ppm). The density was determined using an Anton Paar SY-05 digital densitometer. The freezing point was measured with a Dalian Intelligent DZY-041 freezing point detector, and the volumetric net heat of combustion (VNHOC) was obtained using a Dalian Intelligent DZY-R1B calorimeter. All measurements were performed in triplicate.

2. *Catalyst preparation and characterization*

First, MCM-41/SBA-15 (1.0 g) was dispersed in a toluene solution of 3-mercaptopropyl trimethoxysilane (10 mL) and refluxed for 6 h. The resulting solid was collected by filtration, washed with methanol, and dried at 110 °C for 5 h to yield the thiol-functionalized intermediate. This intermediate was then treated with a 10% H_2O_2 aqueous solution (20 mL) under stirring at 40 °C for 20 h. The final solid product was isolated by filtration, thoroughly washed with distilled water until the filtrate reached neutrality, and dried at 120 °C for 8 h to give the sulfonic acid-functionalized MCM-41/SBA-15 (MCM-41-SO_3H; SBA-15-SO_3H).

Three catalysts including MCM-41, fresh MCM-41-SO_3H, and spent MCM-41-SO_3H were characterized by Fourier transform infrared (FTIR) spectroscopy, and NH_3 temperature-programmed desorption (NH_3-TPD). FTIR spectra were acquired using a Thermo Fisher Scientific Nicolet iS5 spectrometer in the wavenumber range of 4000-400 cm^{-1} to identify framework vibrations and functional groups. Acidity measurements were conducted on a ChemBET Pulsar TPR/TPD chemisorption analyzer (Quantachrome Instruments, USA). In the NH_3-TPD experiments, approximately 0.1 g of each sample was placed in a U-shaped quartz tube and pretreated under an Ar atmosphere at 300 °C for 1 h. After cooling to 100 °C, the sample was exposed to a mixture of NH_3 and He for 1 h to allow ammonia adsorption. The NH_3 flow was then stopped, and the system was purged with He for another hour. Subsequently, the temperature was ramped to 800 °C at a heating rate of 10 °C/min. The desorbed NH_3 was monitored using a thermal conductivity detector (TCD) and the corresponding signal was recorded as a function of temperature.

3. *Catalytic ring-increasing reaction of phenol with terpenes*

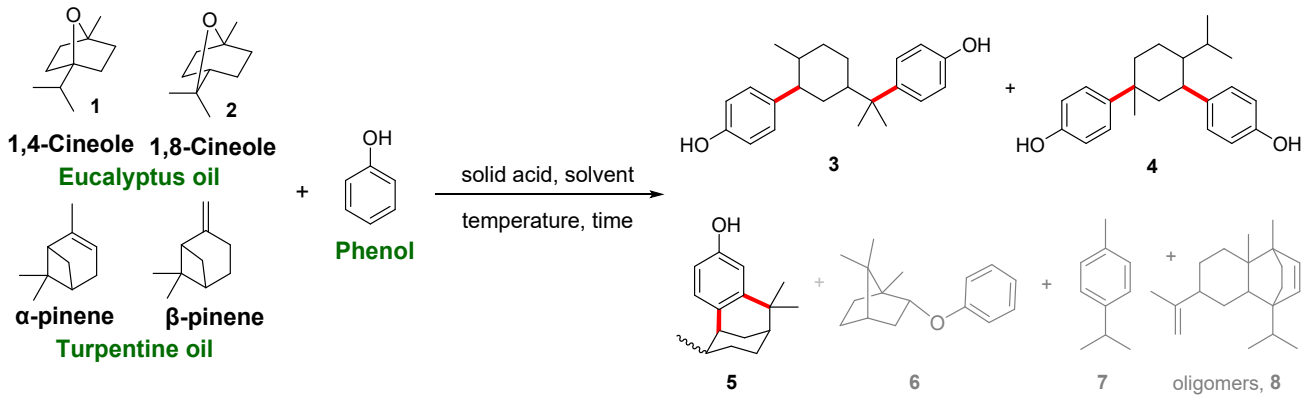

To a 35 mL sealed tube was sequentially added phenol (0.94 g, 10.0 mmol), 1,4-cineole (1.54 g, 10.0 mmol), cyclohexane (1.2 mL) and MCM-41-SO_3H catalyst (123.2 mg). The reaction mixture was stirred at 100 °C for 8 h. Upon completion, the organic phase was diluted with ethyl acetate and further analyzed by gas chromatography (GC, Fuli GCF80 instrument) with tridecane as the internal standard. The GC system was equipped with KB-1 column (30 m, 0.32 mm ID, 0.5 μm film) and a flame ionization detector (FID) using tridecane as the internal standard.

Scale-up experiment: Phenol (18.8 g, 0.2 mol), eucalyptus oil (30.8 g, 0.2 mol), cyclohexane (12 mL), and MCM-41-SO_3H (2.46 g) were added successively into a 200 mL sealed tube. The mixture was stirred at 120 °C and the reaction progress was monitored by GC-MS. Upon completion, the spent MCM-41-SO_3H catalyst was recovered by filtration, washed thoroughly with ethyl acetate, and dried under vacuum. The regenerated catalyst was then used in the next catalytic cycle. The combined organic phase was concentrated by vacuum distillation at 40 °C to recover cyclohexane for reuse. The residual crude mixture was diluted with ethyl acetate, dried over anhydrous $MgSO_4$, and concentrated by rotary evaporation to afford alkylated products as a red liquid.

NMR data of products 3 and 4 (Figures S27 and S28)

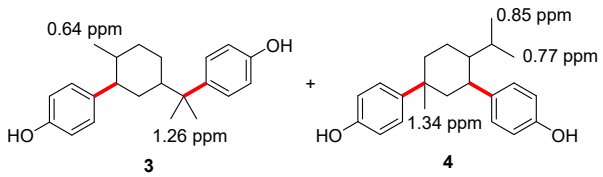

3 **4**

a mixture of **3** and **4**; **3** : **4** = 4.48 : 3 = 1.49 : 1

A mixture of **3** and **4** was obtained with their molar ratio determined by integration of their characteristic ^{1}H NMR signals. **^{1}H NMR** (600 MHz, $CDCl_3$) δ 7.30 – 7.24 (m, 1H), 7.19 (d, *J* = 8.6 Hz, 1H), 7.08 (d, *J* = 8.2 Hz, 1H), 7.00 (d, *J* = 8.3 Hz, 1H), 6.83 – 6.73 (m, 4H), 5.15 (s, 2H), 2.04 – 1.97 (m, 1H), 1.85 – 1.79 (m, 1H), 1.78 – 1.64 (m, 2H), 1.61 – 1.49 (m, 2H), 1.47 – 1.39 (m, 1H), 1.34 (s, 1H), 1.26 (s, 3H), 1.18 – 1.11 (m, 1H), 1.10 – 1.02 (m, 1H), 0.86 (d, *J* = 6.9 Hz, 1H), 0.78 (d, *J* = 6.9 Hz, 1H), 0.65 (d, *J* = 6.4 Hz, 2H). **^{13}C NMR** (150 MHz, $CDCl_3$) δ 153.72, 153.64, 153.33, 153.14, 144.88, 142.34, 139.24, 138.54, 128.66, 127.44, 126.33, 115.43, 115.38, 115.17, 114.93, 114.71, 51.89, 49.50, 48.43, 47.93, 42.95, 39.76, 37.98, 37.67, 37.29, 37.05, 36.07, 27.91, 27.45, 26.08, 25.42, 25.19, 21.61, 20.49, 15.57.

NMR data of product 5 (Figures S29 and S30)

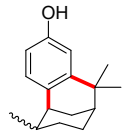

5

multiple diastereoisomers

The presence of multiple quaternary stereocenters gives rise to complex mixtures of diastereoisomers. **^{1}H NMR** (600 MHz, $CDCl_3$) δ 6.98 – 6.87 (m, 1H), 6.74 – 6.64 (m, 2H), 6.17 (s, 1H), 2.79 – 2.01 (m, 3H), 1.92 – 1.40 (m, 5H), 1.28 – 1.18 (m, 2H), 1.12 – 1.04 (m, 1H), 0.96 – 0.58 (m, 7H). **^{13}C NMR** (150 MHz, $CDCl_3$) δ 153.59, 153.56, 153.34, 149.39, 134.85, 131.12, 129.87, 129.15, 128.79, 128.13, 122.76, 115.35, 114.96, 114.68, 112.86, 111.66, 52.39, 47.93, 46.52, 40.97, 39.56, 37.76, 36.77, 36.05, 35.60, 35.06, 34.53, 33.85, 31.69, 29.61, 27.77, 27.32, 26.11, 23.57, 21.80, 21.67, 20.59, 20.12, 19.11, 18.26, 17.29.

NMR data of product 6 (Figures S31 and S32)

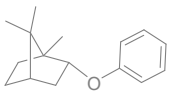

6

^{1}H NMR (600 MHz, $CDCl_3$) δ 7.36 – 6.67 (m, 5H), 4.10 – 3.87 (m, 1H), 1.94 – 1.83 (m, 1H), 1.82 – 1.73 (m, 2H), 1.69 – 1.61 (m, 1H), 1.41 – 1.34 (m, 1H), 1.21 – 1.14 (m, 2H), 1.09 (s, 3H), 1.01 (s, 3H), 0.90 (s, 3H). **^{13}C NMR** (150 MHz, $CDCl_3$) δ 158.12, 129.44, 120.12, 115.54, 84.55, 49.34, 47.17, 45.46, 39.68, 34.40, 27.55, 20.50, 20.29, 11.97.

NMR data of product 9 (Figures S33)

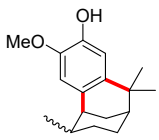

9

multiple diastereoisomers

The presence of multiple quaternary stereocenters gives rise to complex mixtures of diastereoisomers. **^{1}H NMR** (400 MHz, $CDCl_3$) δ 6.90 – 6.53 (m, 2H), 5.40 (s, 1H), 4.14 – 3.43 (m, 3H), 2.29 – 2.01 (m, 3H), 1.80 – 1.46 (m, 5H), 1.32 – 1.18 (m, 2H), 1.03 – 0.57 (m, 8H).

NMR data of product I (Figures S34)

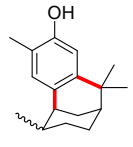

I

multiple diastereoisomers

The presence of multiple quaternary stereocenters gives rise to complex mixtures of diastereoisomers. **^{1}H NMR** (600 MHz, $CDCl_3$) δ 7.04 – 6.84 (m, 1H), 6.76 – 6.62 (m, 1H), 5.51 – 5.16 (m, 1H), 2.89 – 2.33 (m, 1H), 2.28 – 2.15 (m, 3H), 1.99 – 1.43 (m, 5H), 1.39 – 1.15 (m, 5H), 1.11 – 0.59 (m, 6H).

NMR data of product II (Figures S35)

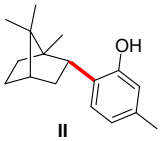

II

multiple diastereoisomers

The presence of multiple quaternary stereocenters gives rise to complex mixtures of diastereoisomers. **^{1}H NMR** (600 MHz, $CDCl_3$) δ 7.28 – 7.02 (m, 1H), 6.88 – 6.53 (m, 2H), 5.02 – 4.72 (m, 1H), 2.46 – 2.24 (m, 4H), 1.98 – 1.24 (m, 8H), 1.21 – 0.79 (m, 8H).

NMR data of product III (Figures S36)

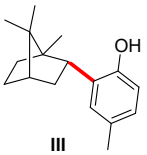

III

multiple diastereoisomers

The presence of multiple quaternary stereocenters gives rise to complex mixtures of diastereoisomers. **^{1}H NMR** (600 MHz, $CDCl_3$) δ 7.25 – 6.98 (m, 1H), 6.98 – 6.63 (m, 2H), 5.43 – 4.68 (m, 1H), 2.57 – 2.17 (m, 4H), 2.10 – 0.68 (m, 16H).

4. *Catalytic hydrodeoxygenation of alkylated products*

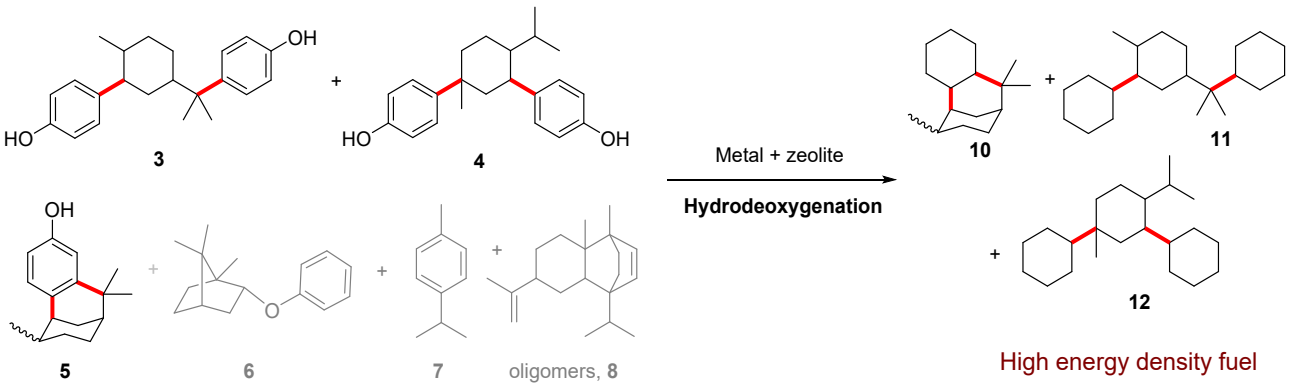

Alkylated products (280.0 mg), Pd/C (metal content 5%, 14.0 mg), H-Y (14.0 mg), and cyclohexane (2.0 mL) were sequentially charged into a 100 mL autoclave reactor. The mixture was stirred at 180 °C under 3.5 MPa of H_2 for 10 h. After cooling down to room temperature, the yield of fuel was determined by Fuli GC F80 equipped with KB-1 column (30 m, 0.32 mm ID, 0.5 μm film) and a flame ionization detector (FID) using tridecane as the internal standard. To assess the potential for practical application, the reusability of Pd/C and H-Y catalysts was investigated. After each run, the catalyst mixture was recovered by centrifugation, thoroughly washed with methanol, and then directly reused in the subsequent cycle.

Scale-up experiment: Alkylated products (30 g), Pd/C (metal content 5%, 3.0 g), H-Y (3.0 g) and cyclohexane (40 mL) were successively added into a 100 mL autoclave reactor. The mixture was stirred at 180 °C, during which hydrogen is continuously introduced to maintain the system pressure. The reaction process was monitored by GC-MS. When no further decrease in hydrogen pressure was observed, Pd/C and H-Y catalysts were separated by filtration and used in the subsequent cycle. A final vacuum distillation (vacuum oil pump and bath temperature of 120 °C) gave rise to the target tricyclic fuel.

5. *Copies of GC chromatograms*

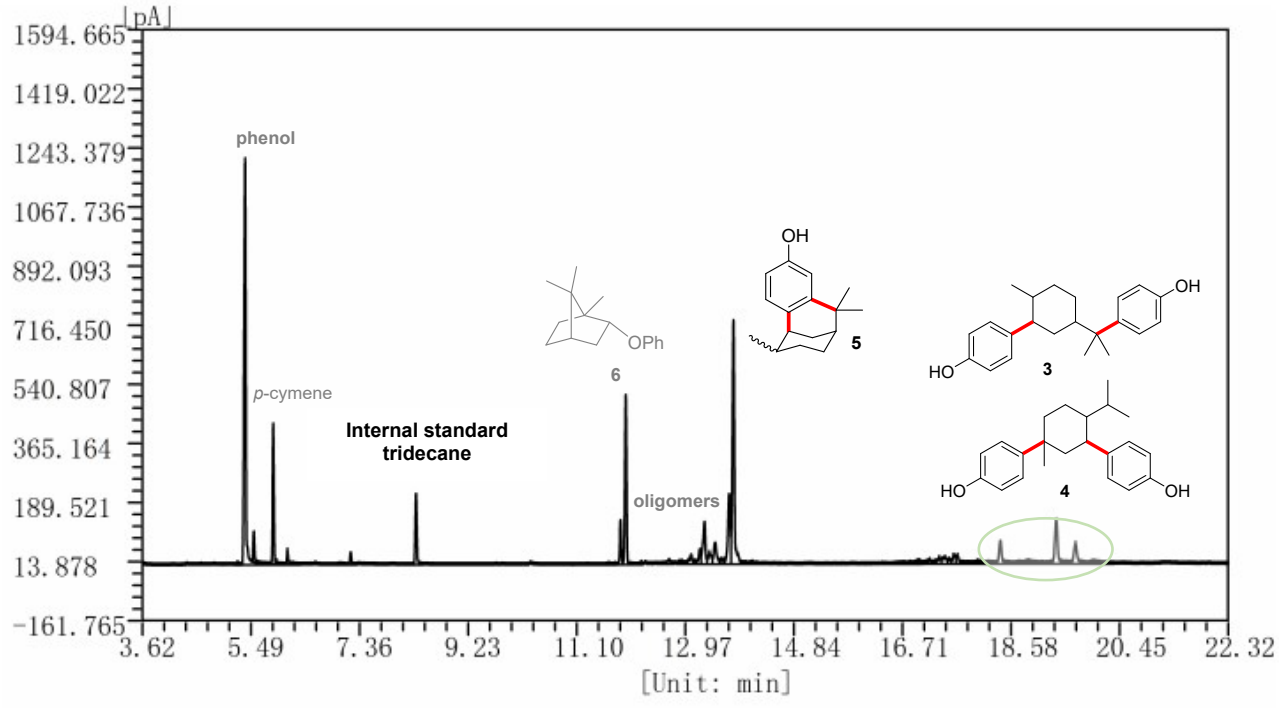

Figure S1. Gas chromatogram of the products from ring-increasing reaction between phenol and 1,4-cineole. Reaction conditions: phenol (0.94 g, 10.0 mmol), 1,4-cineole (1.54 g, 10.0 mmol), MCM-41-SO_3H (0.1232 g), cyclohexane (1.2 mL), 100 °C for 8 h.

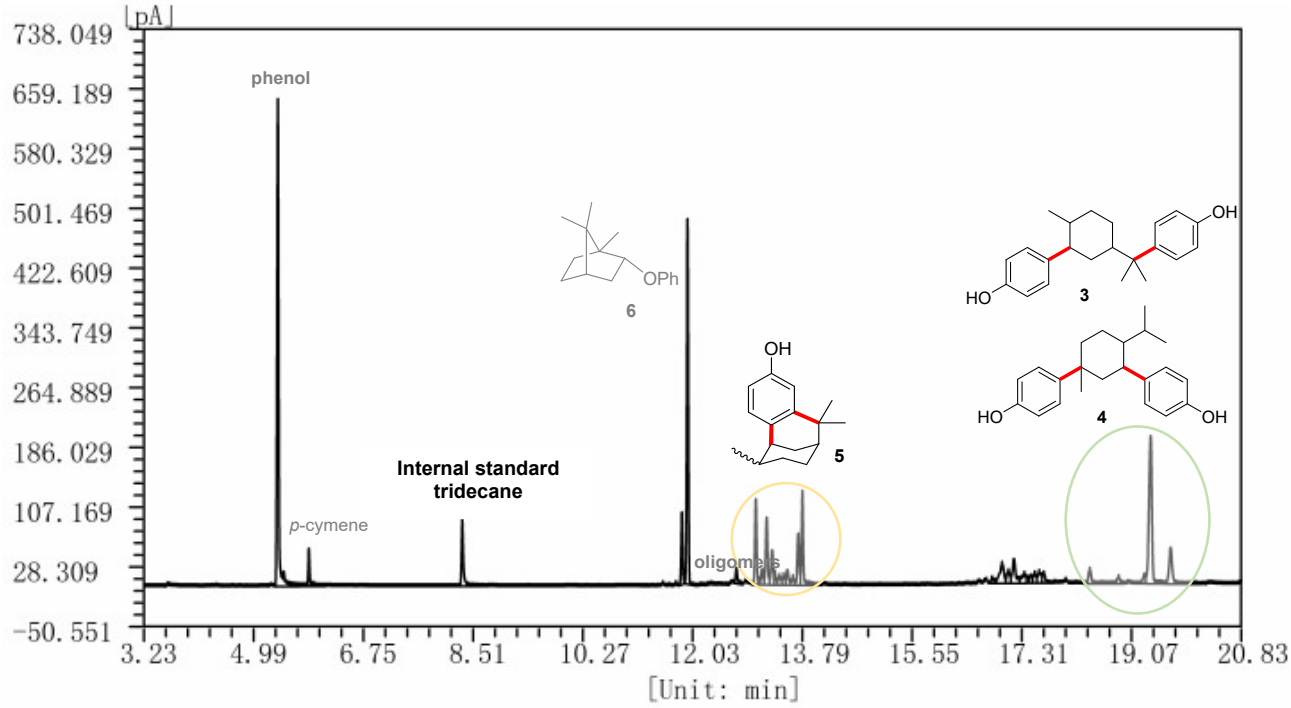

Figure S2. Gas chromatogram of the products from ring-increasing reaction between phenol and 1,8-cineole. Reaction conditions: phenol (0.94 g, 10.0 mmol), 1,8-cineole (1.54 g,10.0 mmol), MCM-41-SO_3H (0.1232 g), cyclohexane (1.2 mL), 100 °C for 8 h.

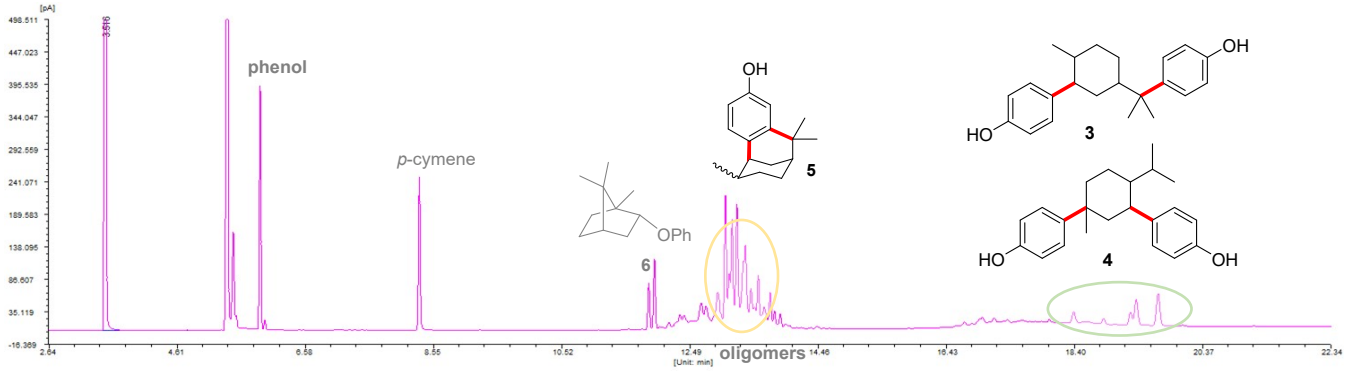

Figure S3. Gas chromatogram of the products from ring-increasing reaction between phenol and crude eucalyptus oil. Reaction conditions: phenol (0.94 g, 10.0 mmol), crude eucalyptus oil (1.54 g, 10.0 mmol), MCM-41-SO_3H (0.1232 g), cyclohexane (1.2 mL), 100 °C for 8 h.

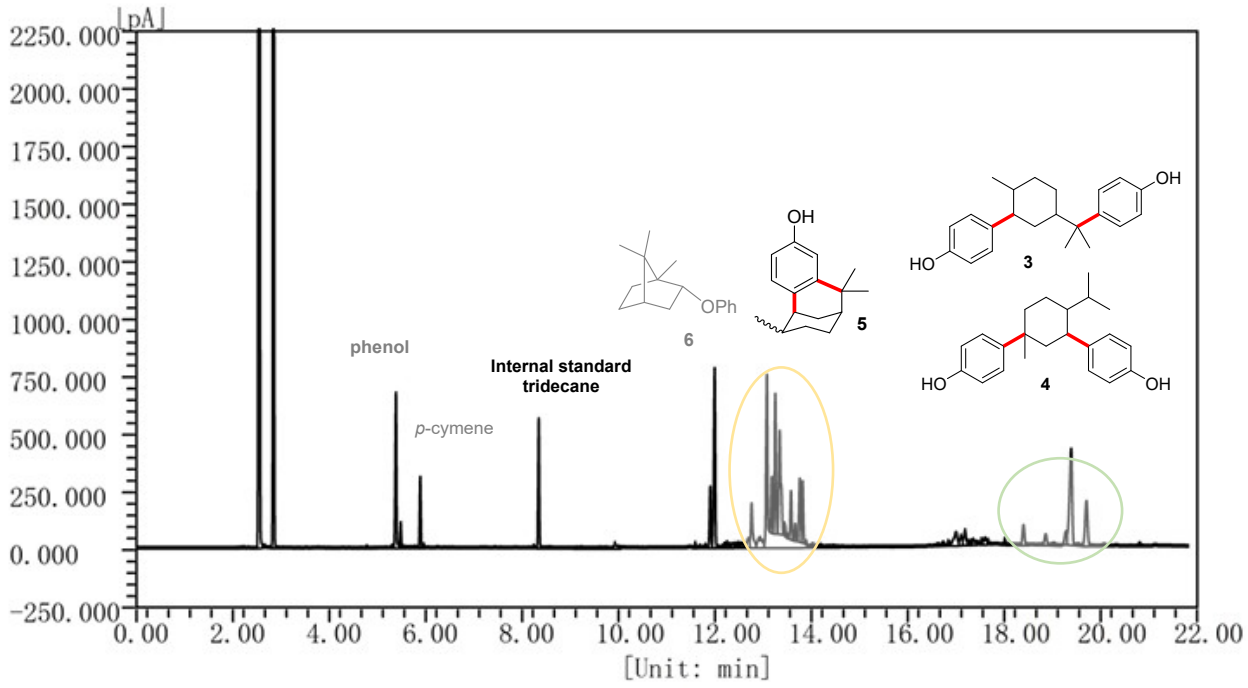

Figure S4. Gas chromatogram of the products from ring-increasing reaction between phenol and limonene. Reaction conditions: limonene (1.36 g, 10.0 mmol), phenol (0.94 g, 10.0 mmol), MCM-41-SO_3H (0.109 g), cyclohexane (1.2 mL), 100 °C for 8 h.

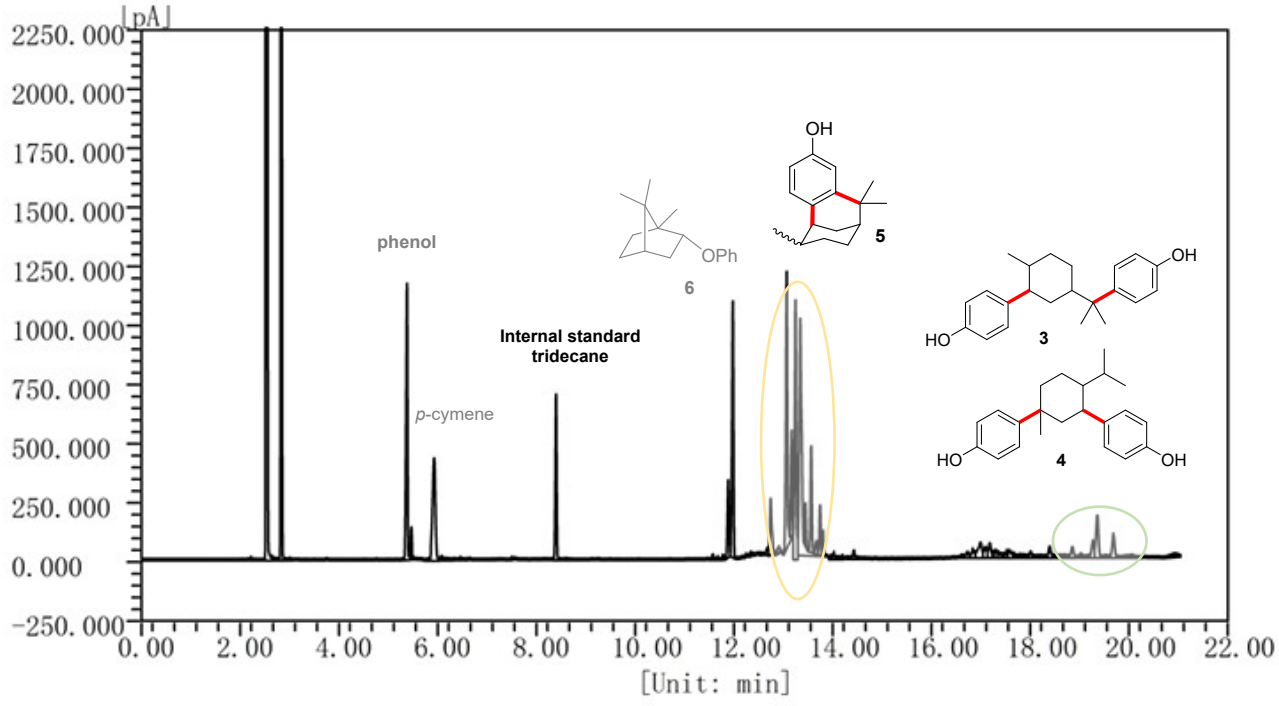

Figure S5. Gas chromatogram of the products from ring-increasing reaction between phenol and α-terpinene. Reaction conditions: α-terpinene (1.36 g, 10.0 mmol), phenol (0.94 g, 10.0 mmol), MCM-41-SO_3H (0.109 g), cyclohexane (1.2 mL), 100 °C for 8 h.

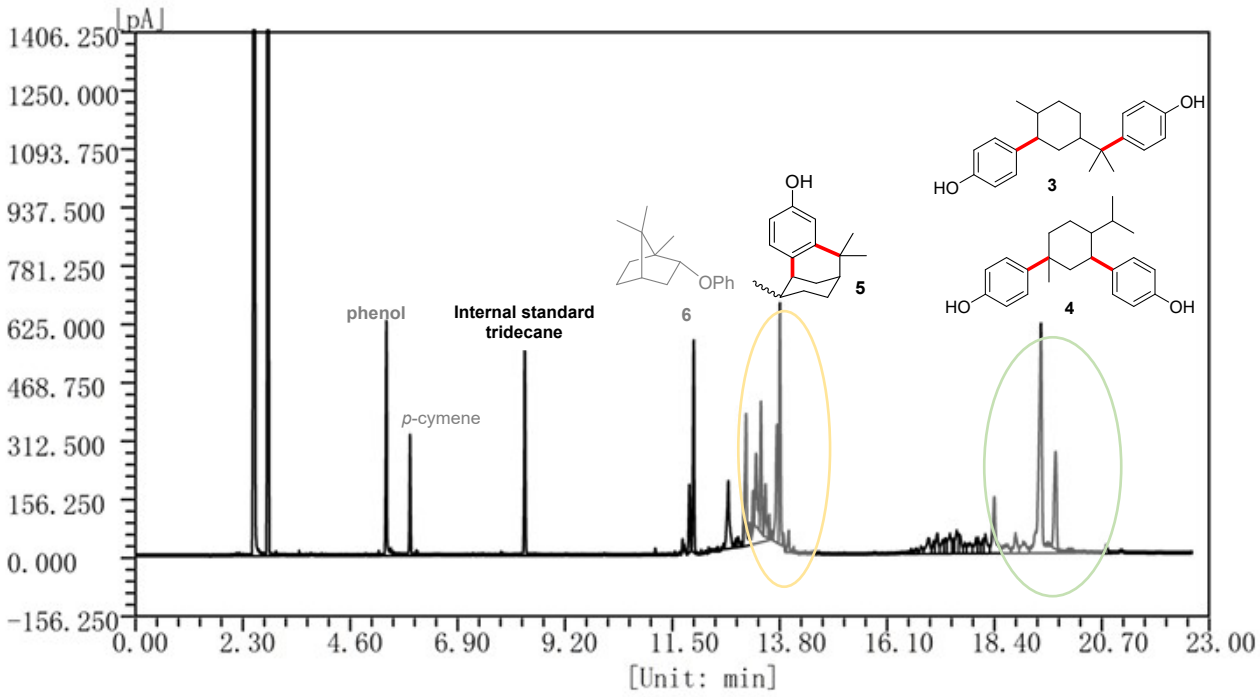

Figure S6. Gas chromatogram of the products from alkylation reaction between phenol and α-pinene. Reaction conditions: terpinolene (1.36 g, 10.0 mmol), phenol (0.94 g, 10.0 mmol), MCM-41-SO_3H (0.109 g), cyclohexane (1.2 mL), 100 °C for 8 h.

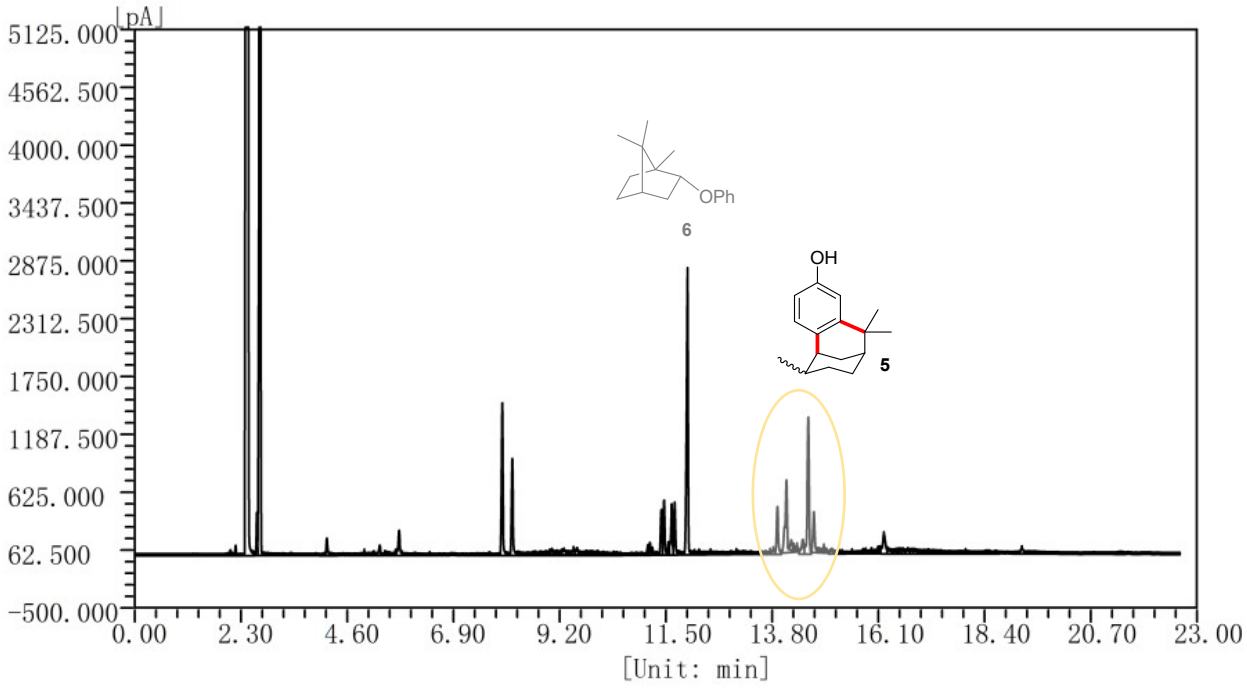

Figure S7. Gas chromatogram of the products from alkylation reaction between phenol and isoprene. Reaction conditions: isoprene (1.36 g, 20.0 mmol), phenol (0.94 g, 10.0 mmol), MCM-41-SO_3H (0.109 g), cyclohexane (1.2 mL), 100 °C for 8 h.

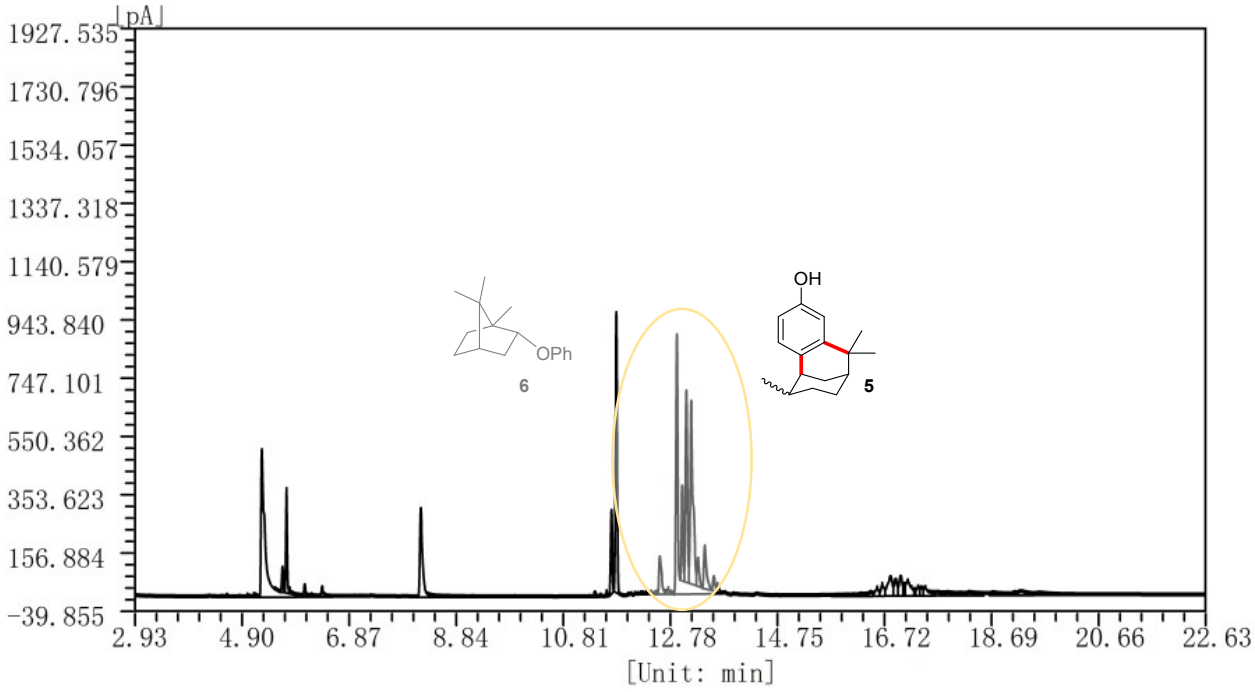

Figure S8. Gas chromatogram of the products from alkylation reaction between phenol and α-terpineol. Reaction conditions: α-terpineol (1.54 g, 10.0 mmol), phenol (0.94 g, 10.0 mmol), MCM-41-SO_3H (0.123 g), cyclohexane (1.2 mL), 100 °C for 8 h.

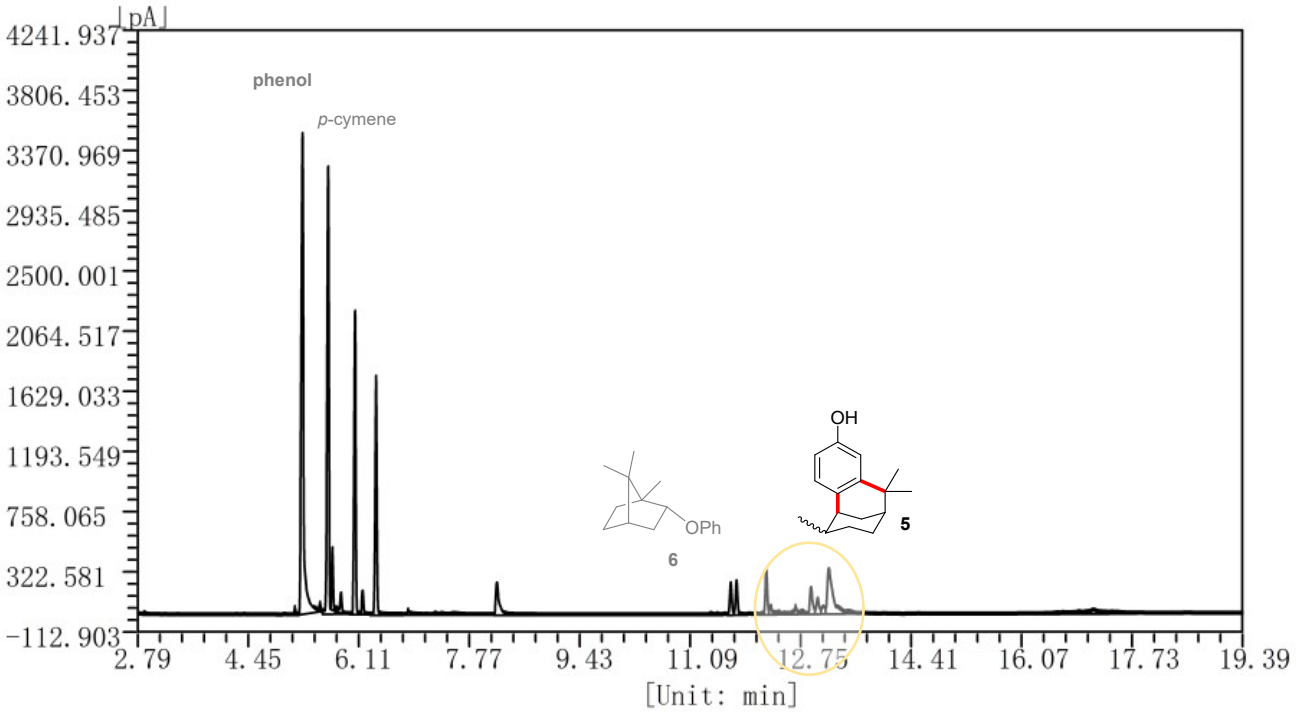

Figure S9. Gas chromatogram of the products from alkylation reaction between phenol and 4-terpineol. Reaction conditions: 4-terpineol (1.54 g, 10.0 mmol), phenol (0.94 g, 10.0 mmol), MCM-41-SO_3H (0.123 g), cyclohexane (1.2 mL), 100 °C for 8 h.

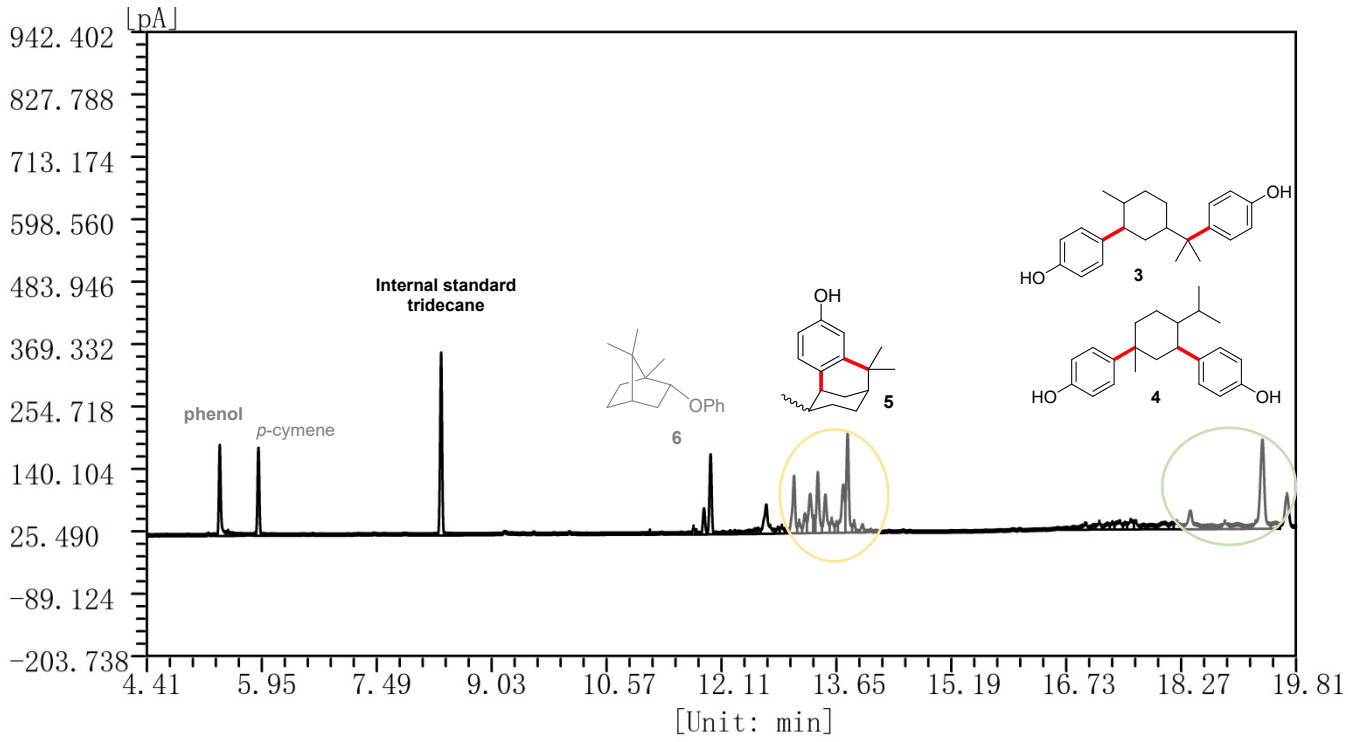

Figure S10. Gas chromatogram of the products from ring-increasing reaction between phenol and turpentine oil. Reaction conditions: phenol (0.94 g, 10.0 mmol), turpentine oil (1.36 g,10.0 mmol), Nafion (0.109 g), cyclohexane (1.2 mL), 100 °C for 8 h.

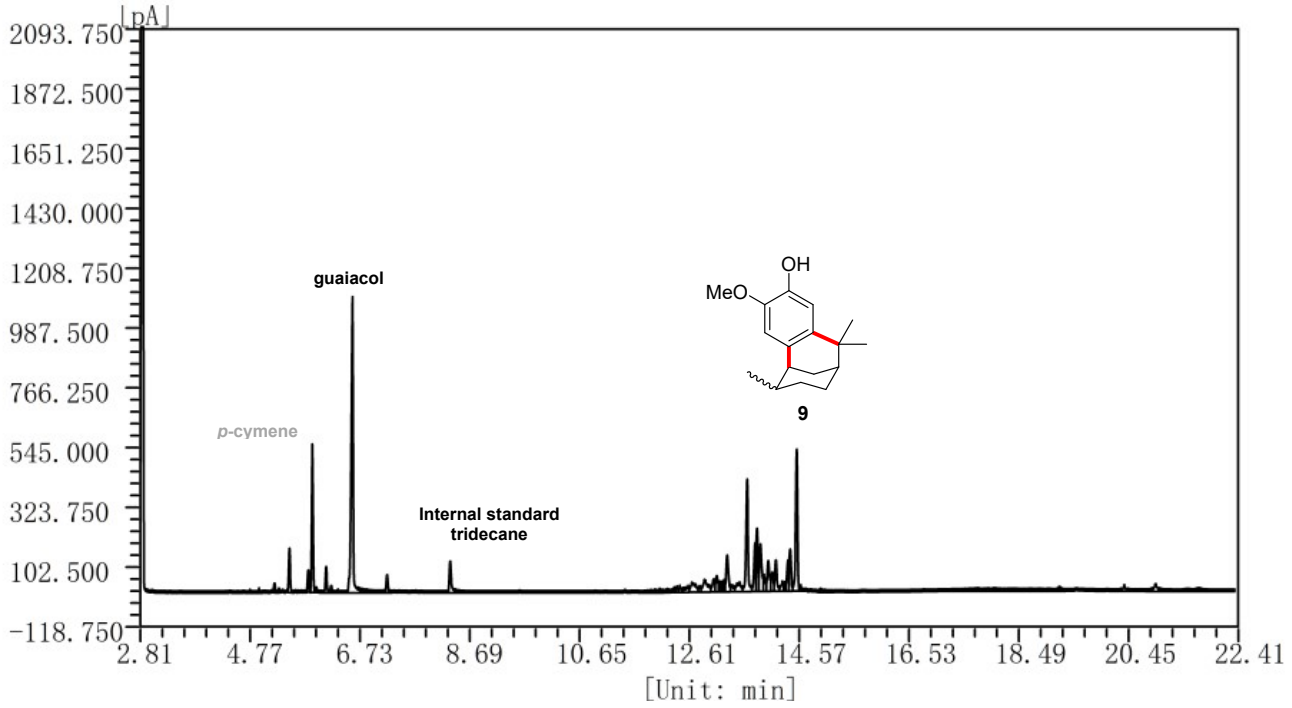

Figure S11. Gas chromatogram of the products from ring-increasing reaction between guaiacol and crude eucalyptus oil. Reaction conditions: guaiacol (1.24 g, 10.0 mmol), crude eucalyptus oil (1.54 g, 10.0 mmol), MCM-41-SO_3H (0.1232 g), cyclohexane (1.2 mL), 100 °C for 8 h.

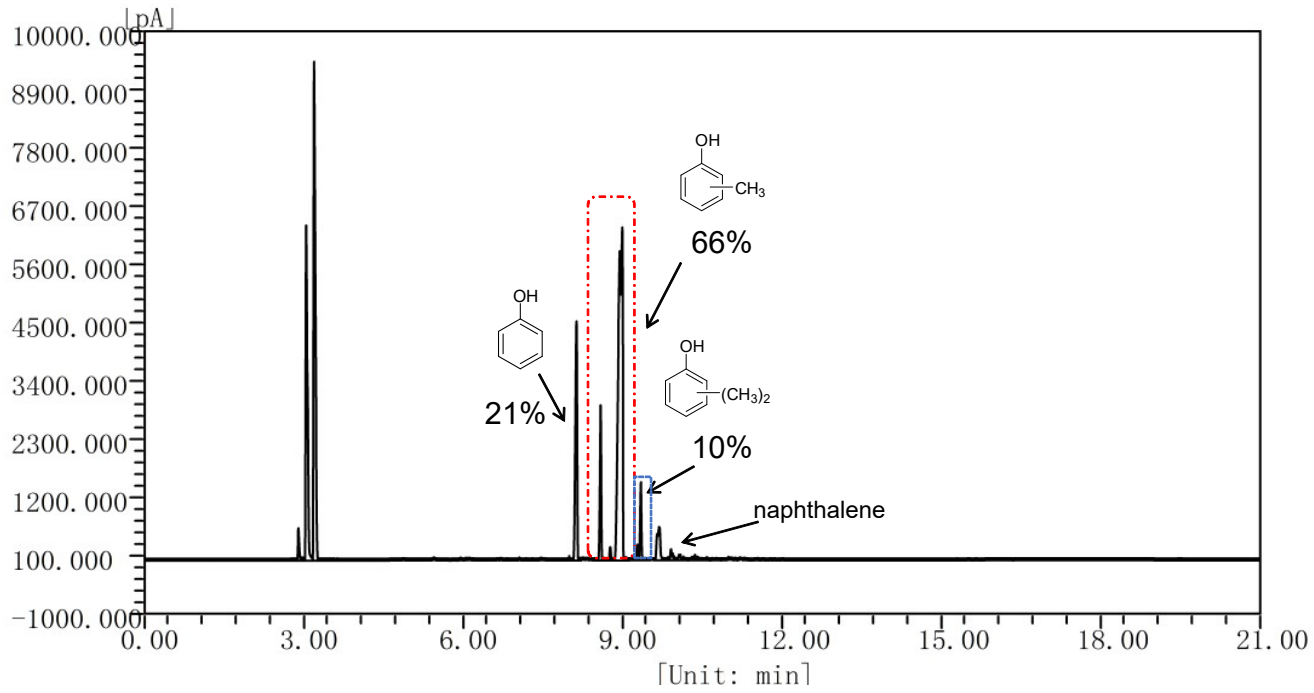

Figure S12. Gas chromatogram of crude phenolic mixture derived from coal tar.

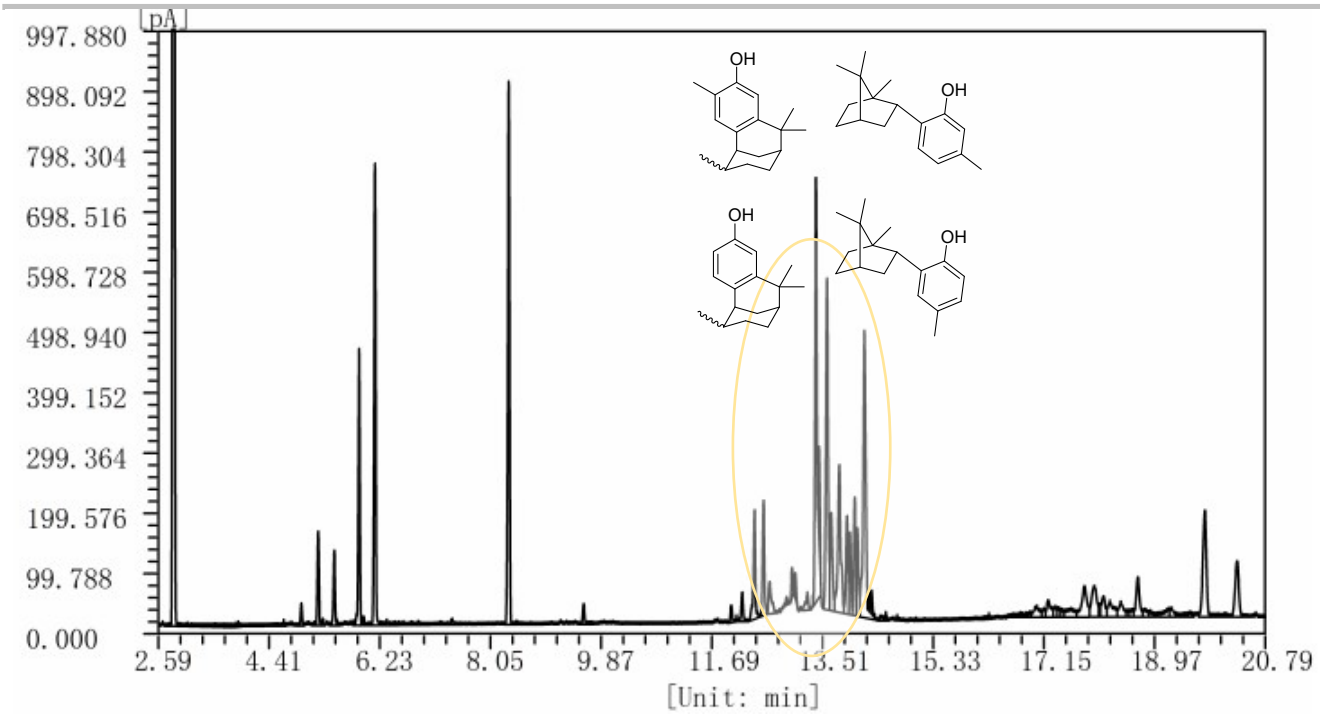

Figure S13. Gas chromatogram of ring-increasing reaction between crude phenolic mixture and turpentine oil.

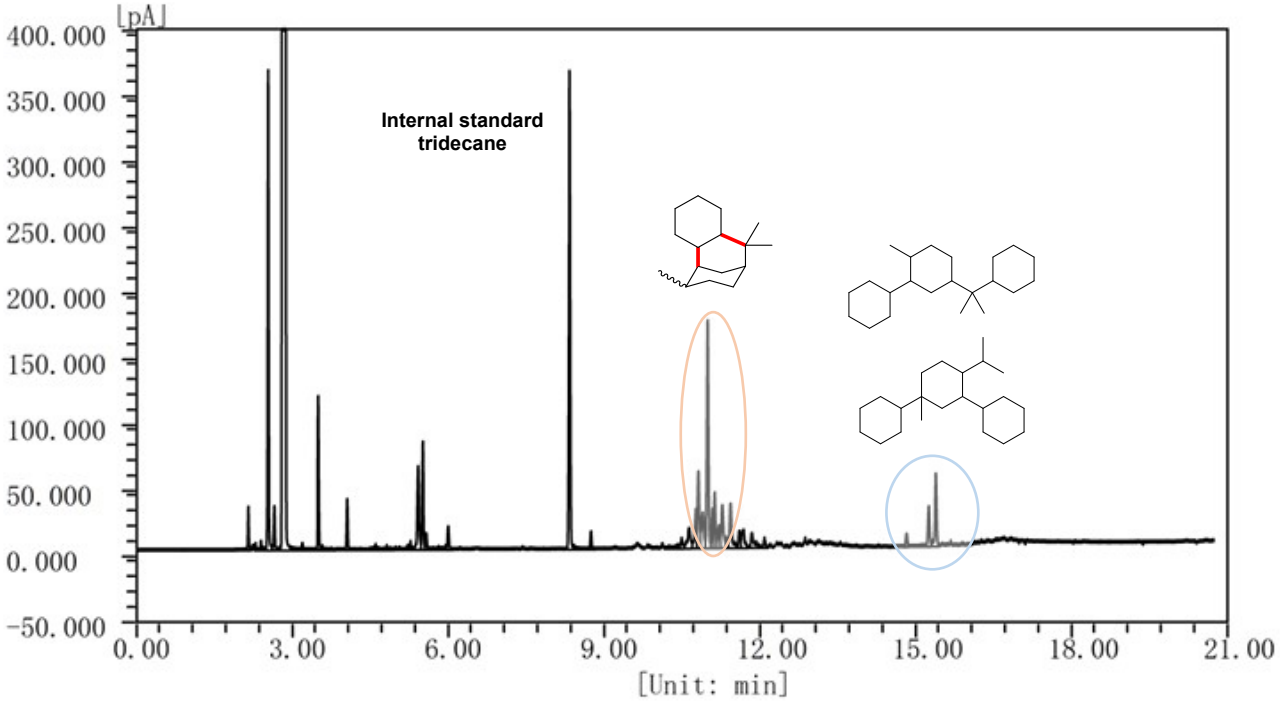

Figure S14. Gas chromatogram of HDO products using phenol and eucalyptus oil as feedstocks.

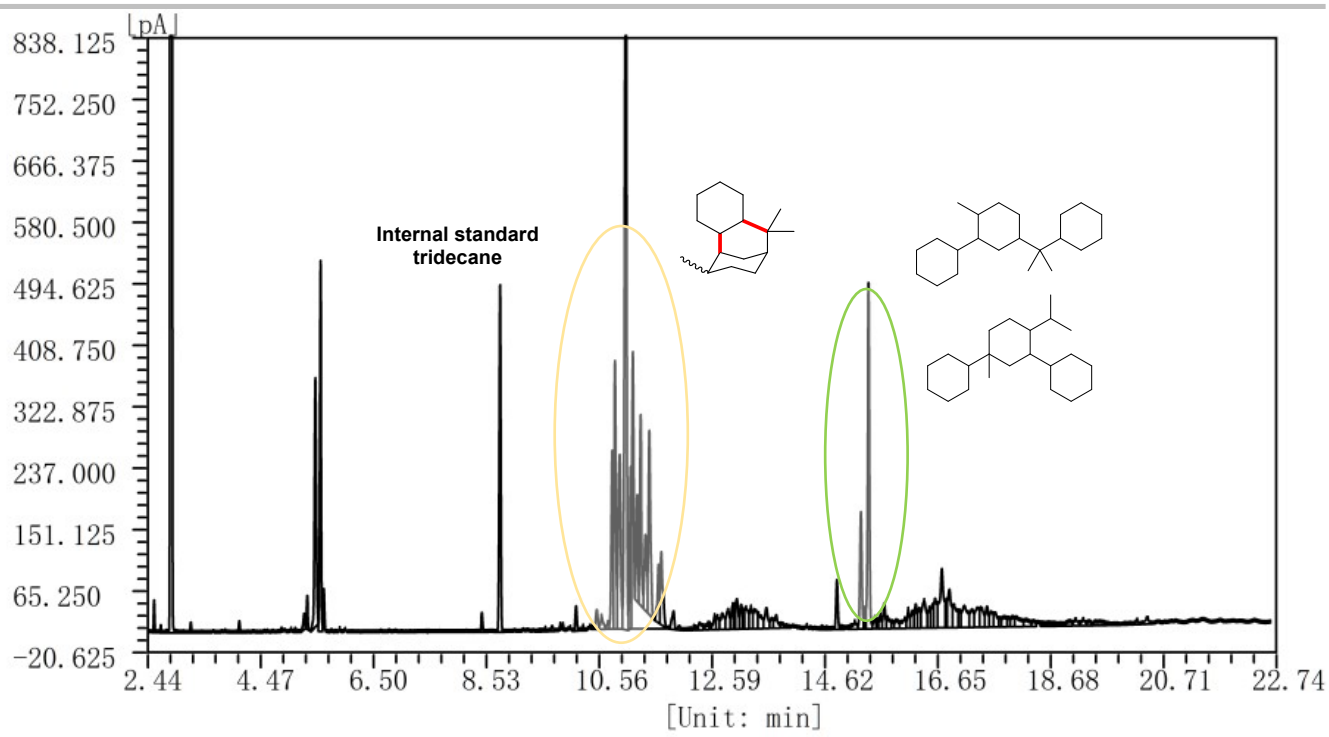

Figure S15. Gas chromatogram of HDO products using phenol and turpentine oil as feedstocks.

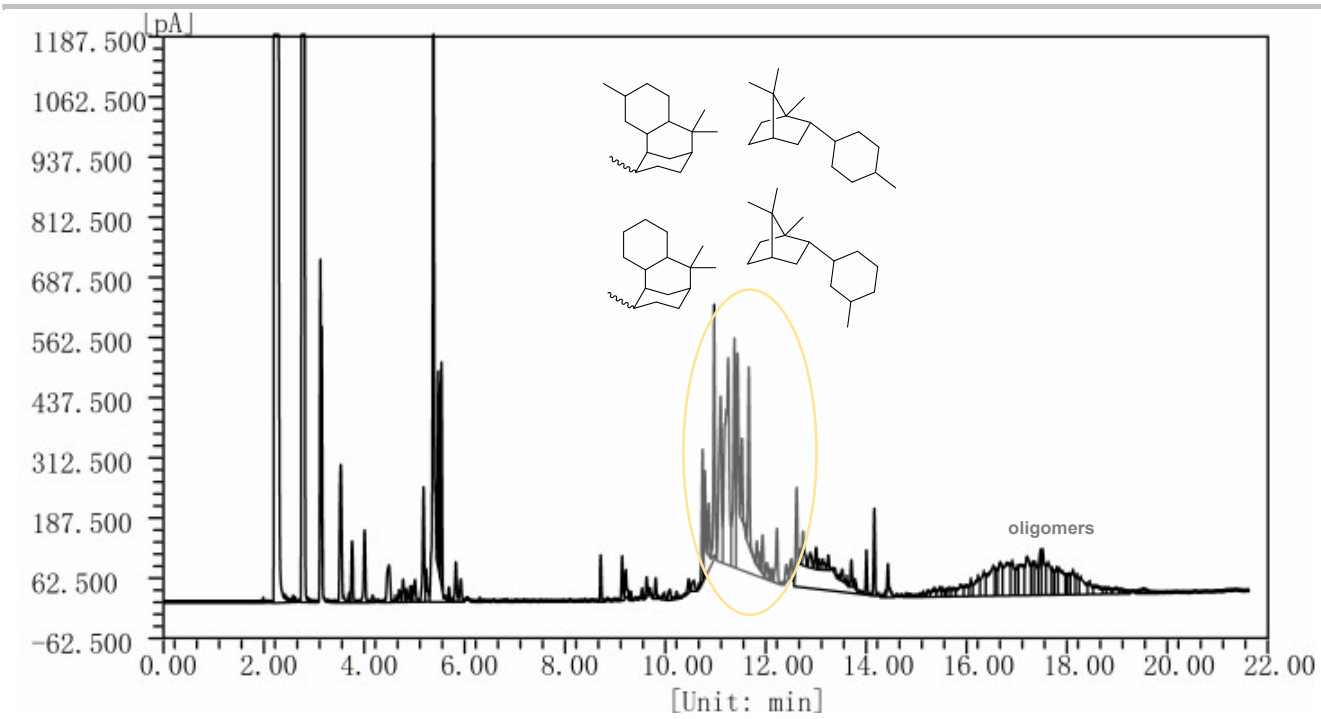

Figure S16. Gas chromatogram of HDO products using crude phenolic mixture and turpentine oil as feedstocks.

6. *Copies of MS spectra*

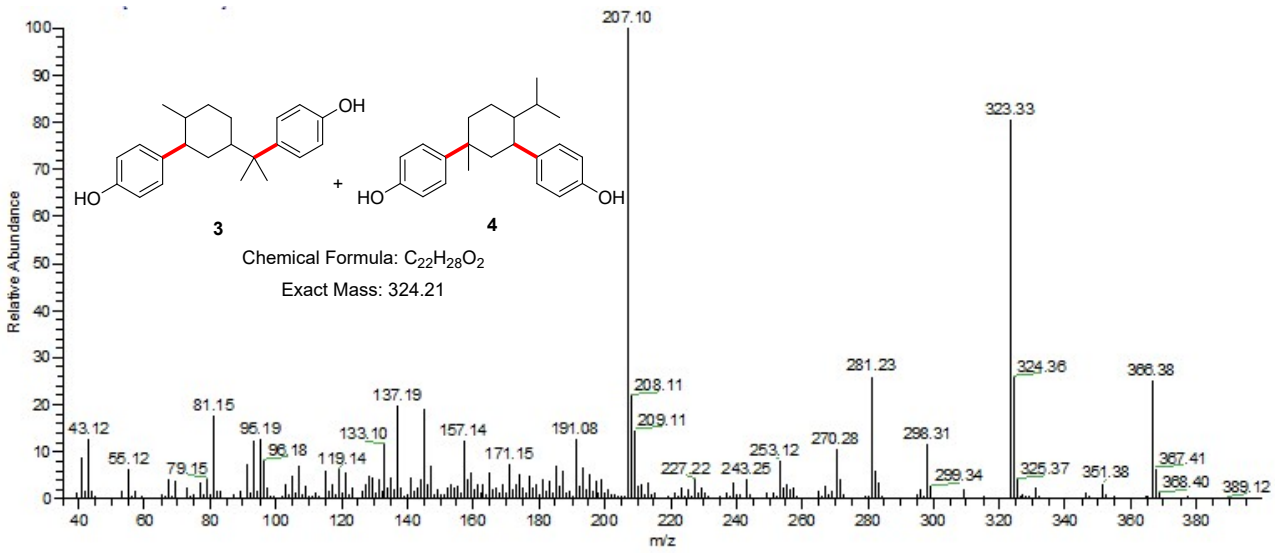

Figure S17. MS spectrum of products **3** and **4**.

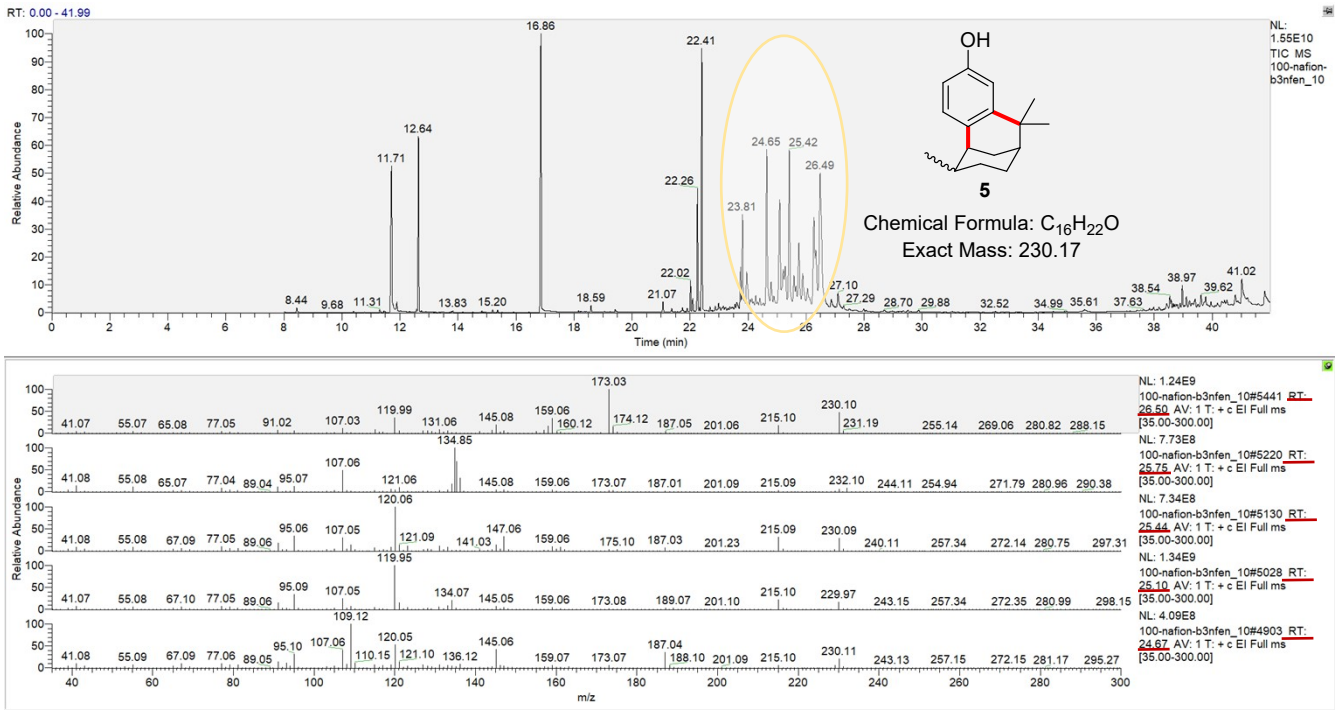

Figure S18. MS spectrum of product **5** (multiple diastereoisomers).

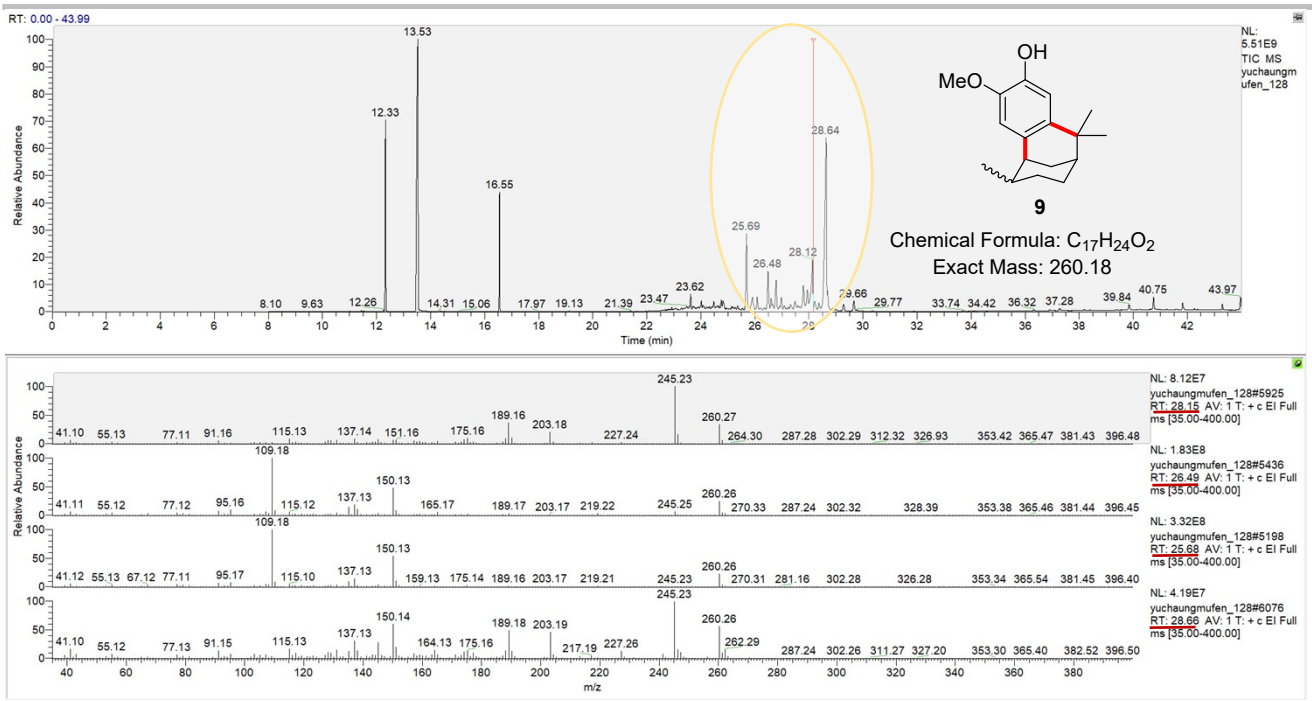

Figure S19. MS spectrum of product **9** (multiple diastereoisomers).

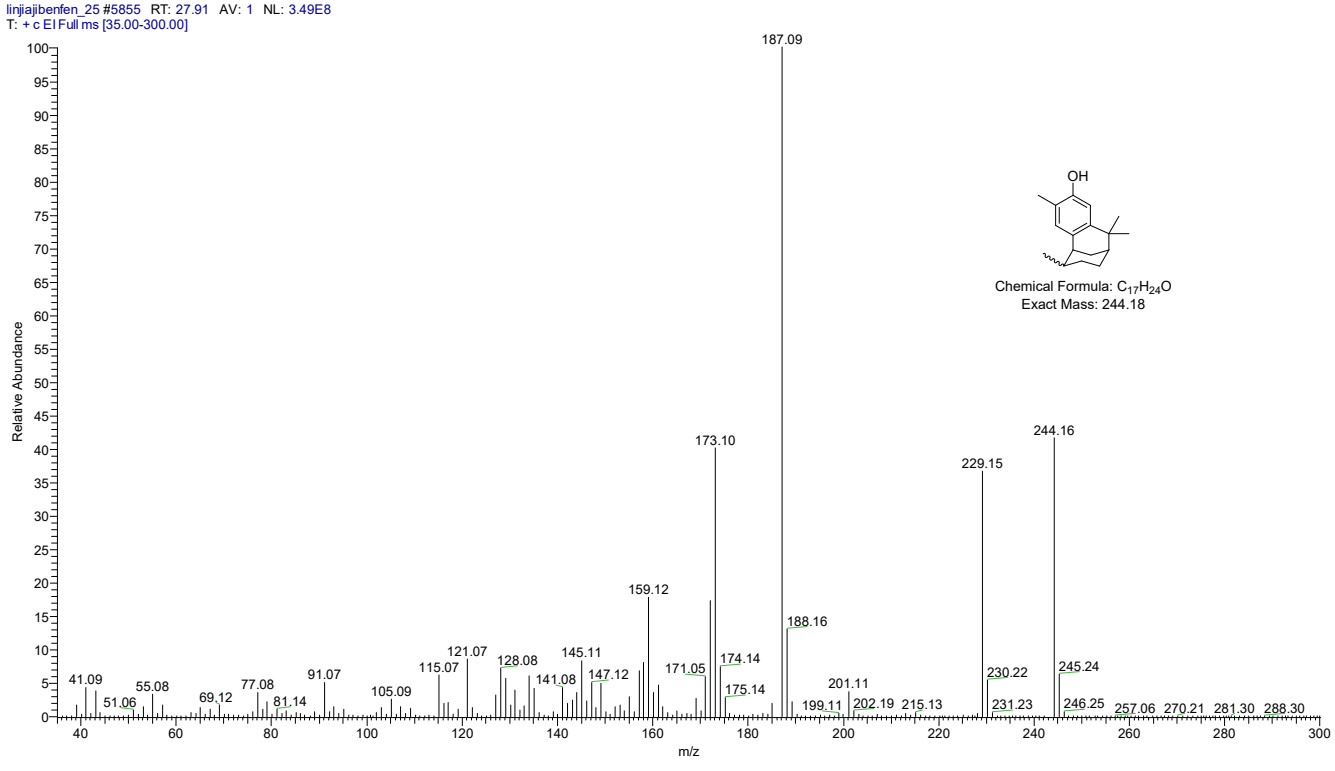

Figure S20. MS spectrum of product **I**.

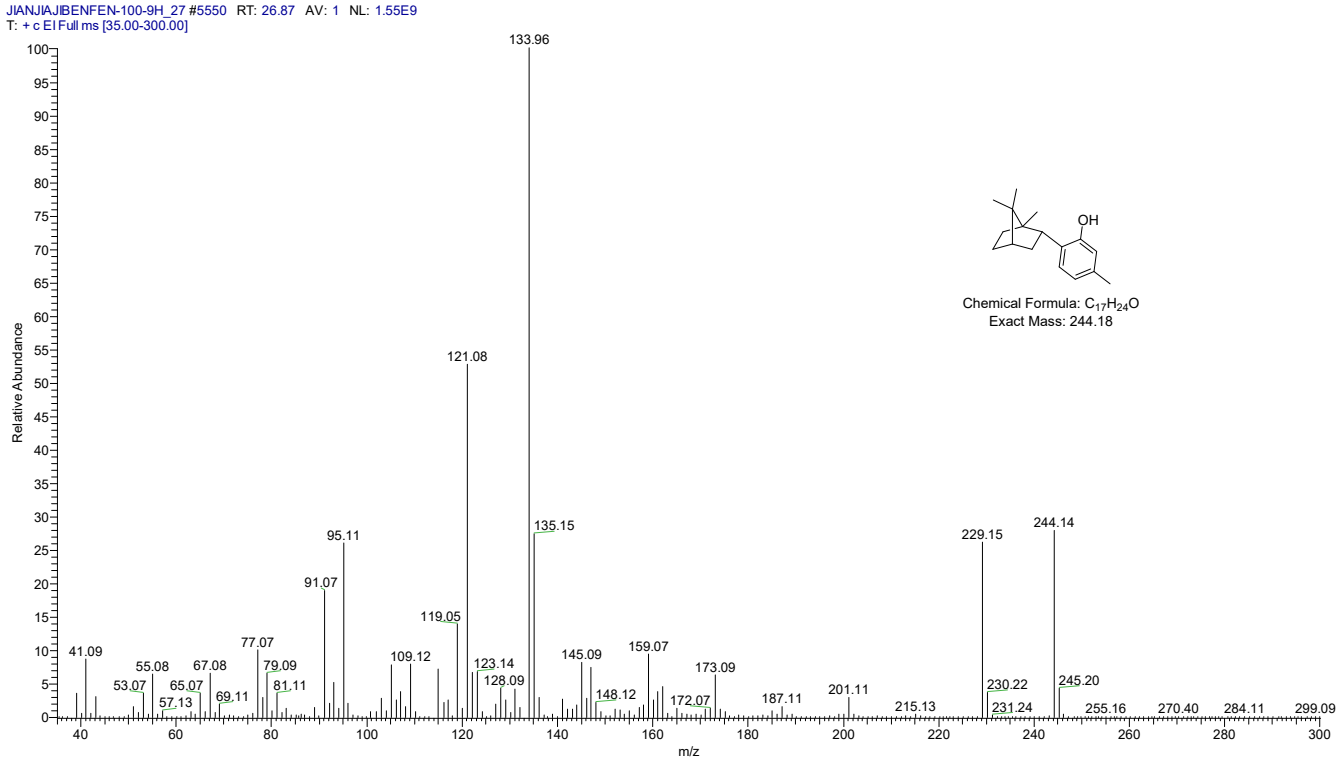

Figure S21. MS spectrum of product **II**.

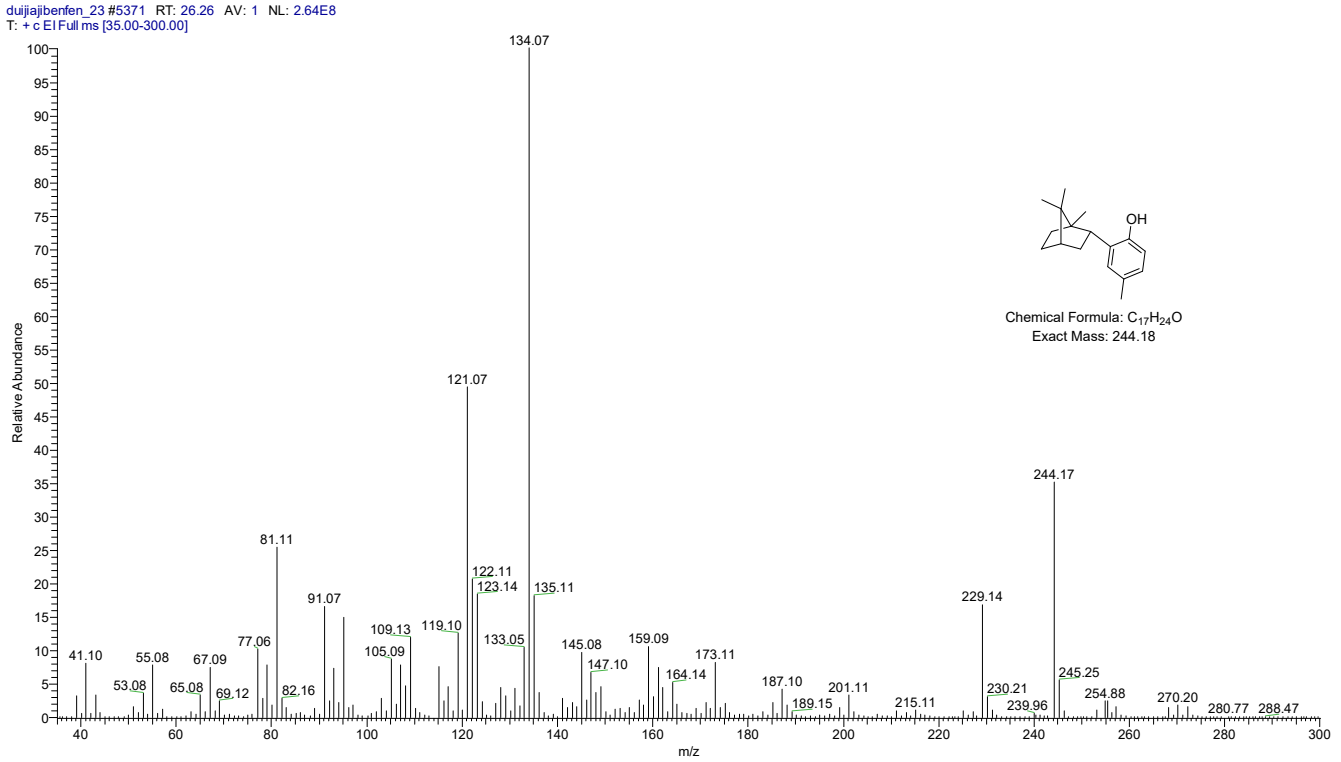

Figure S22. MS spectrum of product **III**.

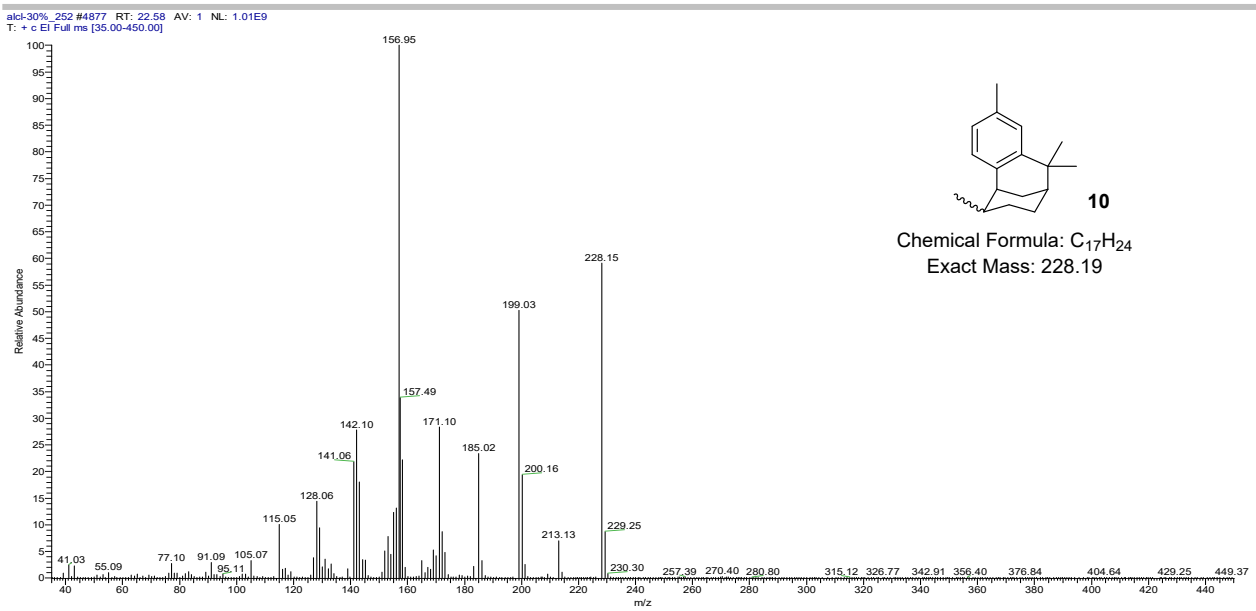

Figure S23. MS spectrum of products **10**.

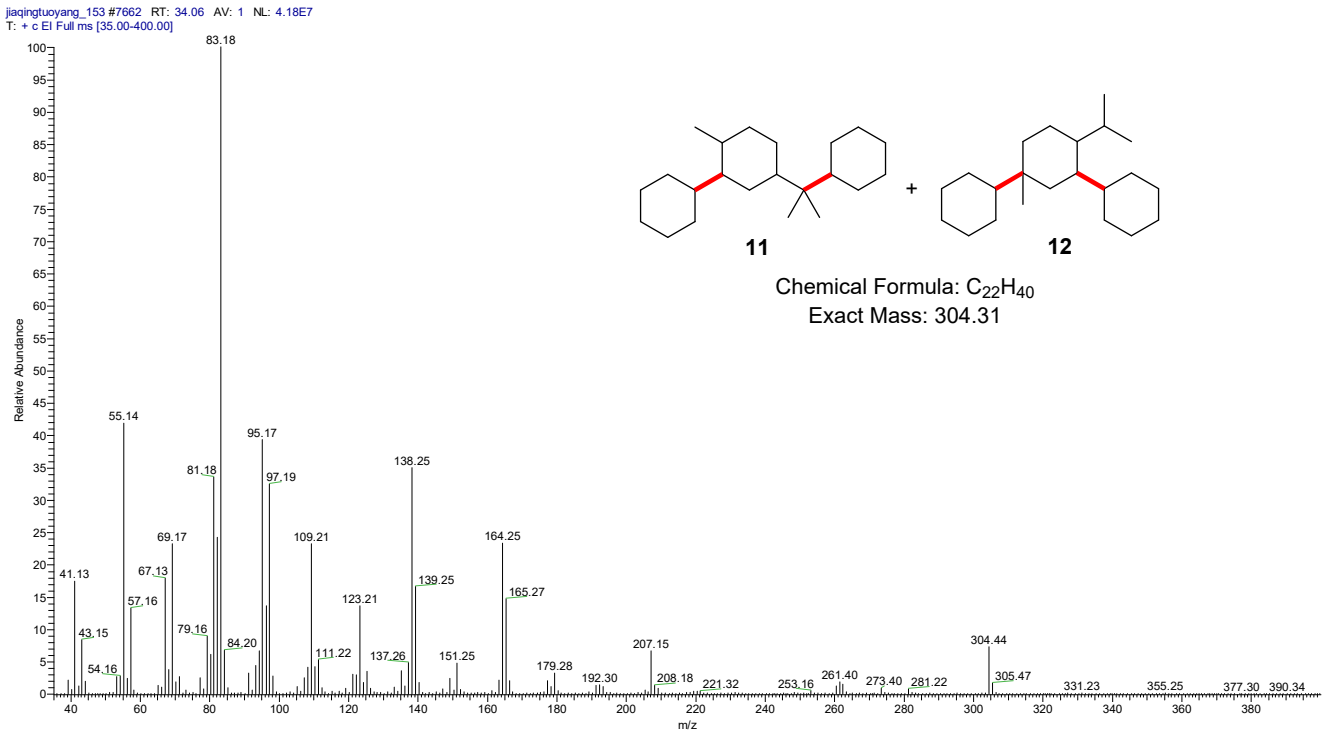

Figure S24. MS spectrum of products **11** and **12**.

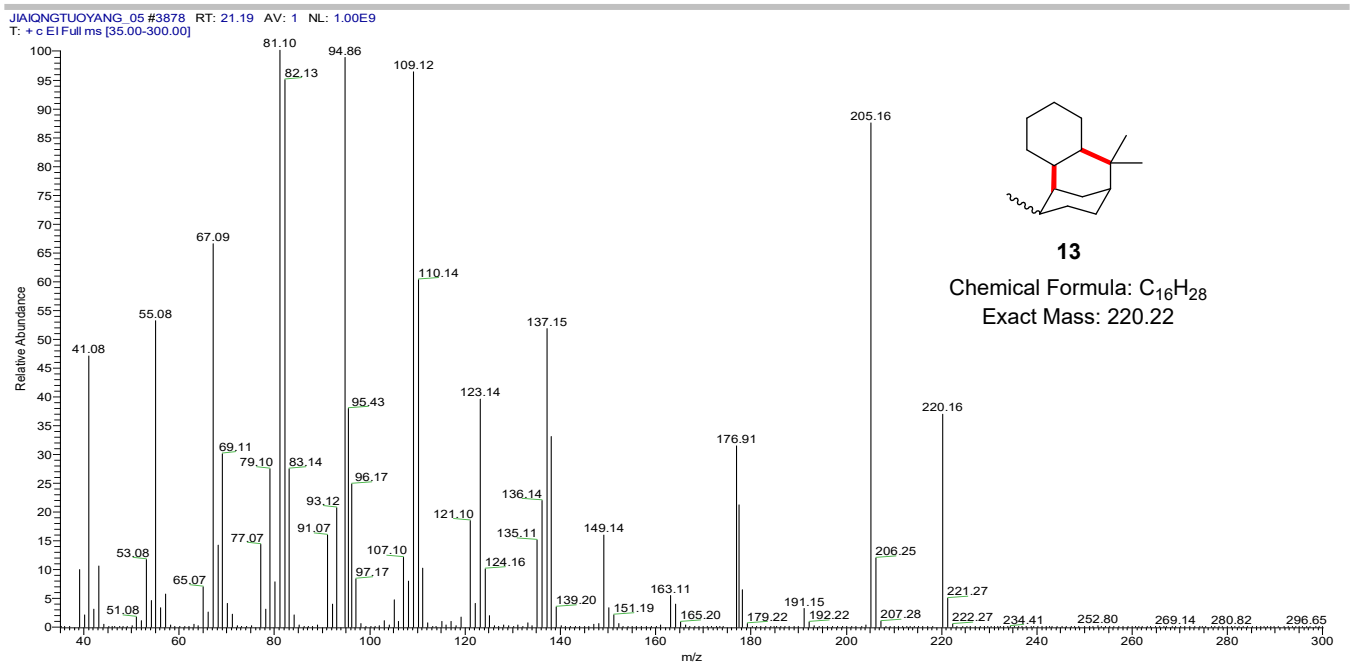

Figure S25. MS spectrum of product **12**.

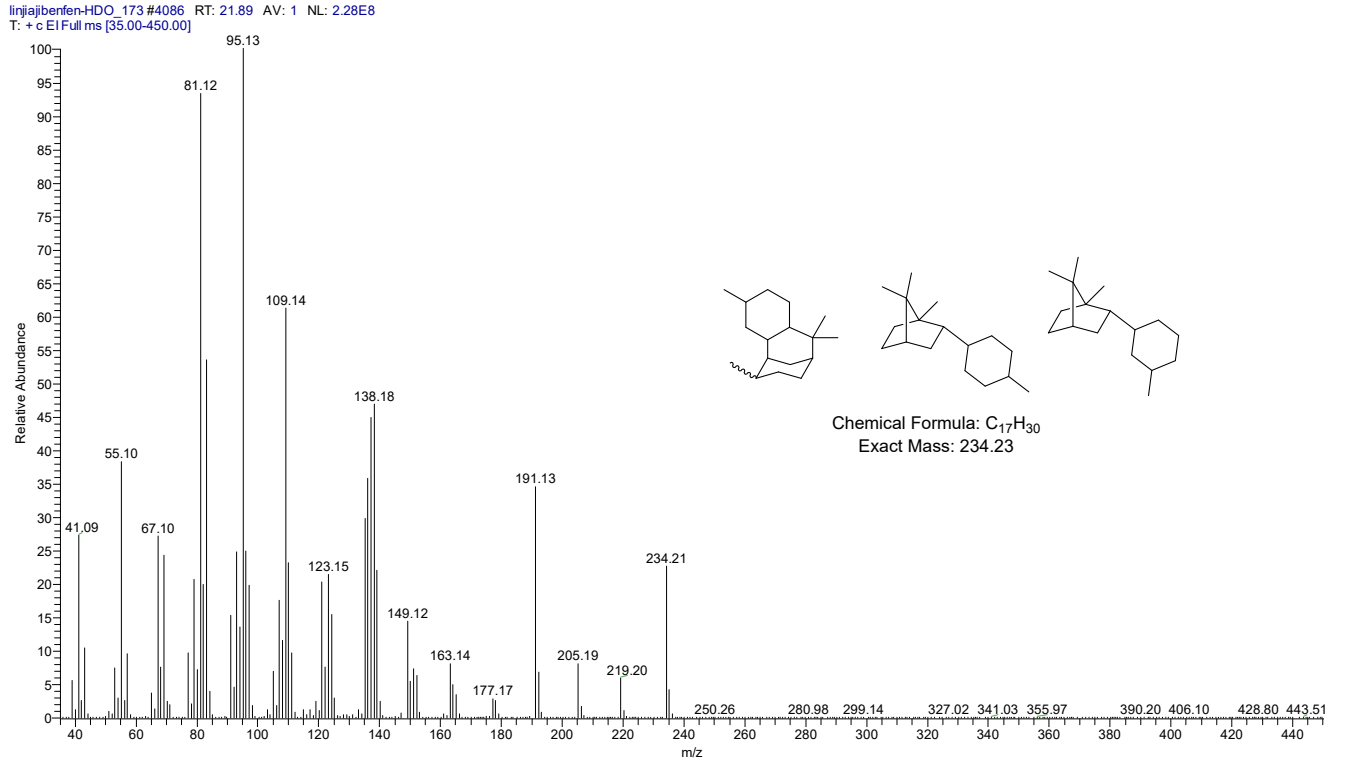

Figure S26. MS spectrum of HDO products using crude phenolic mixture and turpentine oil as feedstocks.

7. *Copies of NMR spectra*

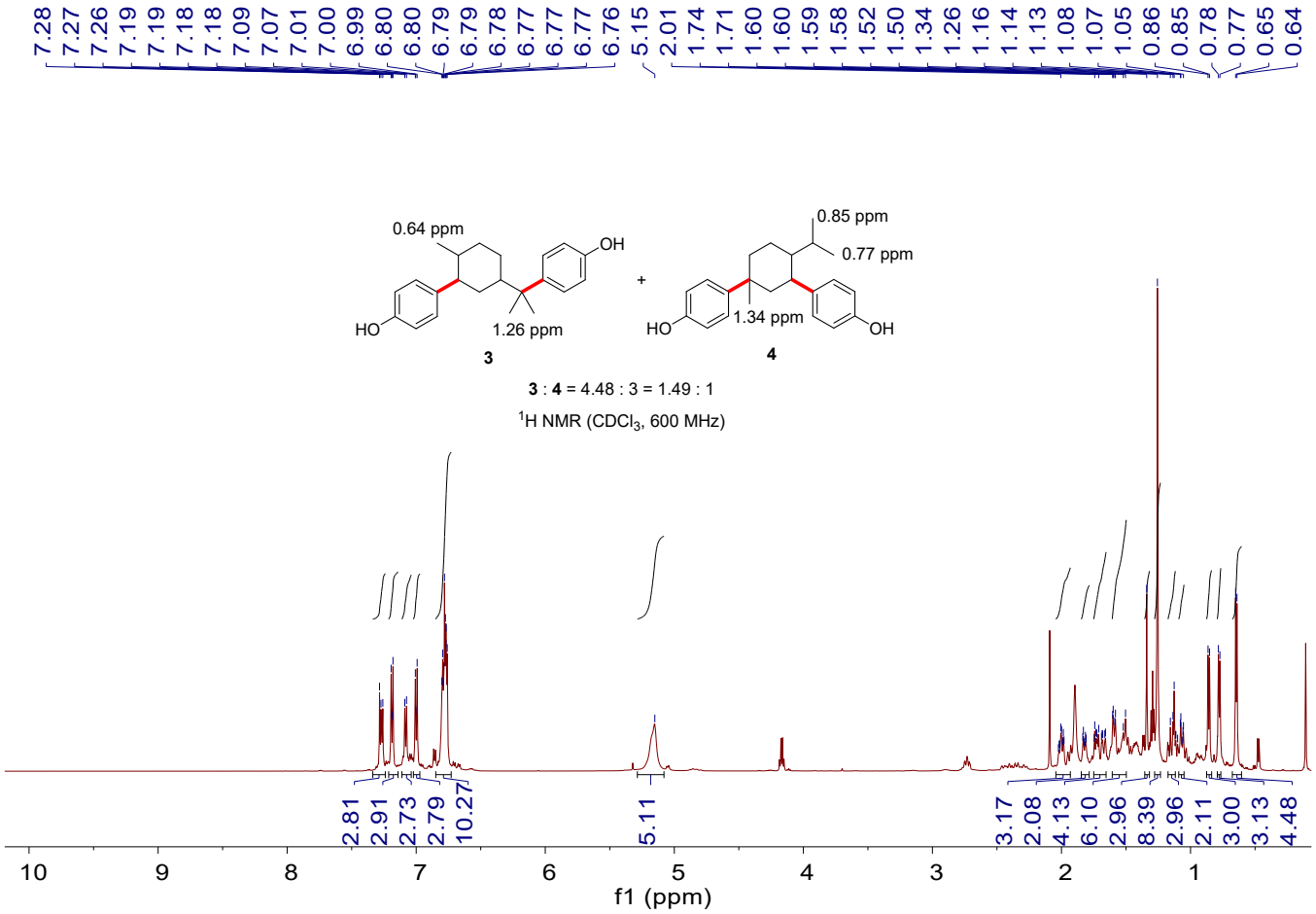

Figure S27. ^{1}H NMR spectrum of products **3** and **4**.

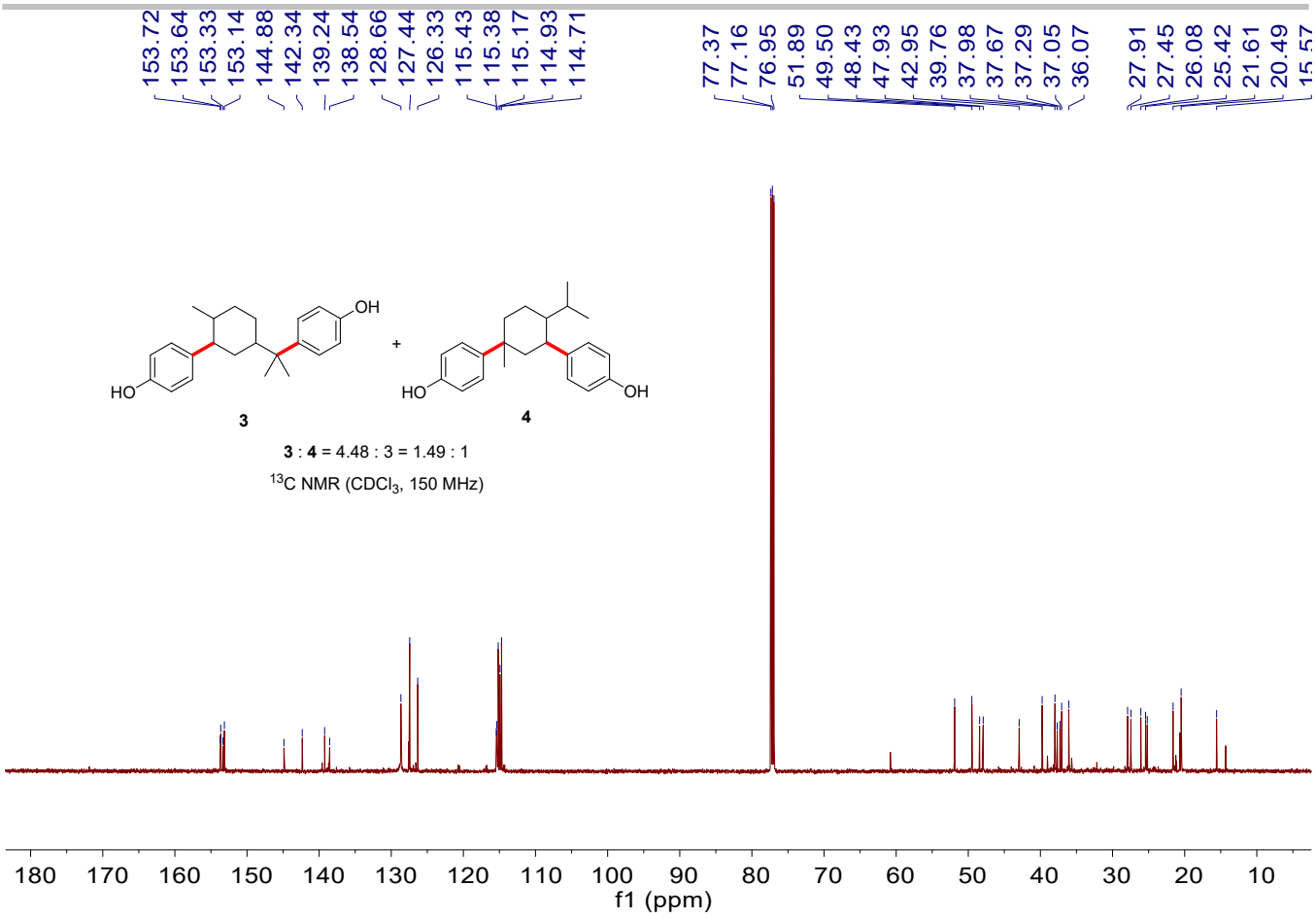

Figure S28. ^{13}C NMR spectrum of products **3** and **4**.

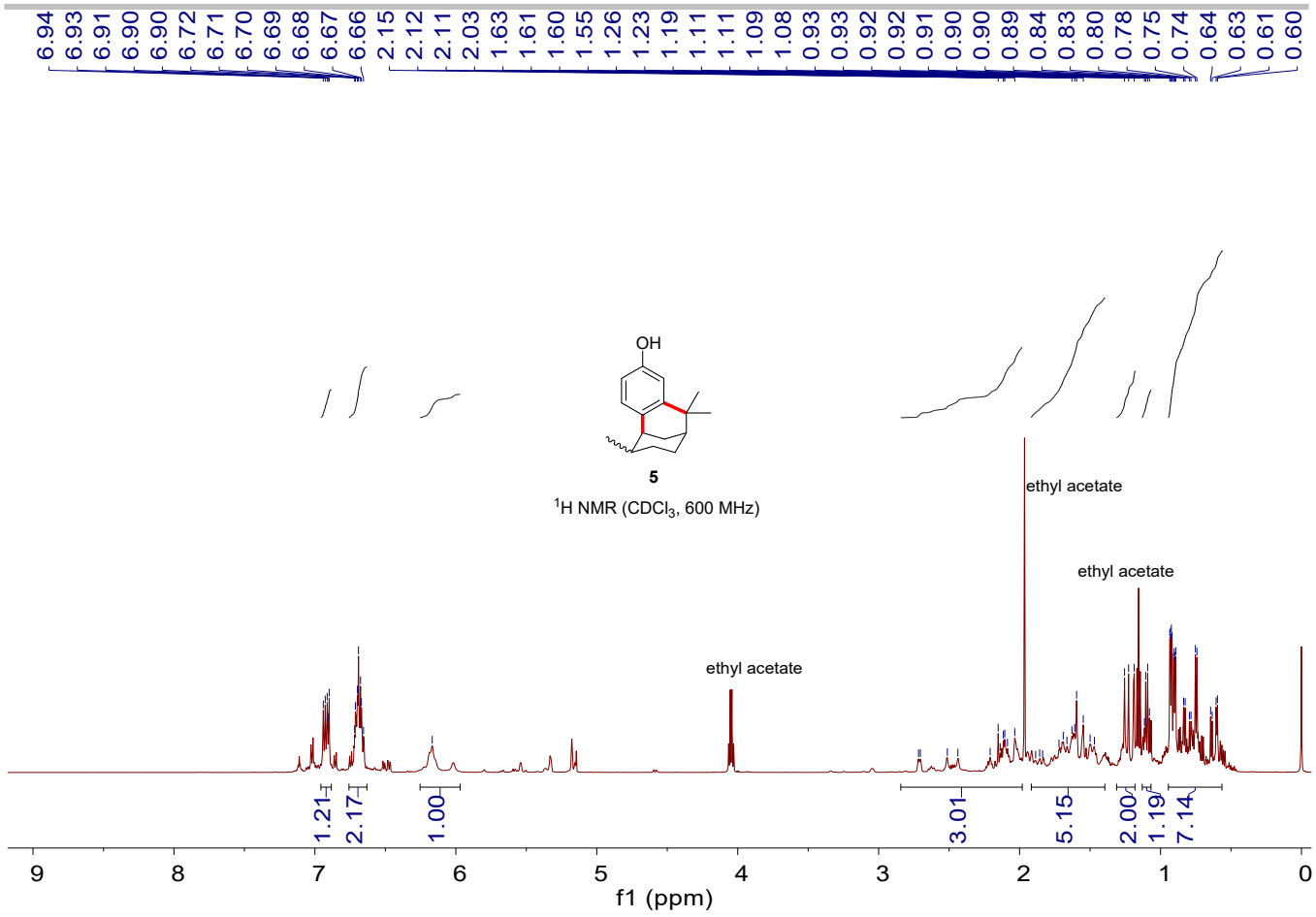

Figure S29. ^{1}H NMR spectrum of product **5**.

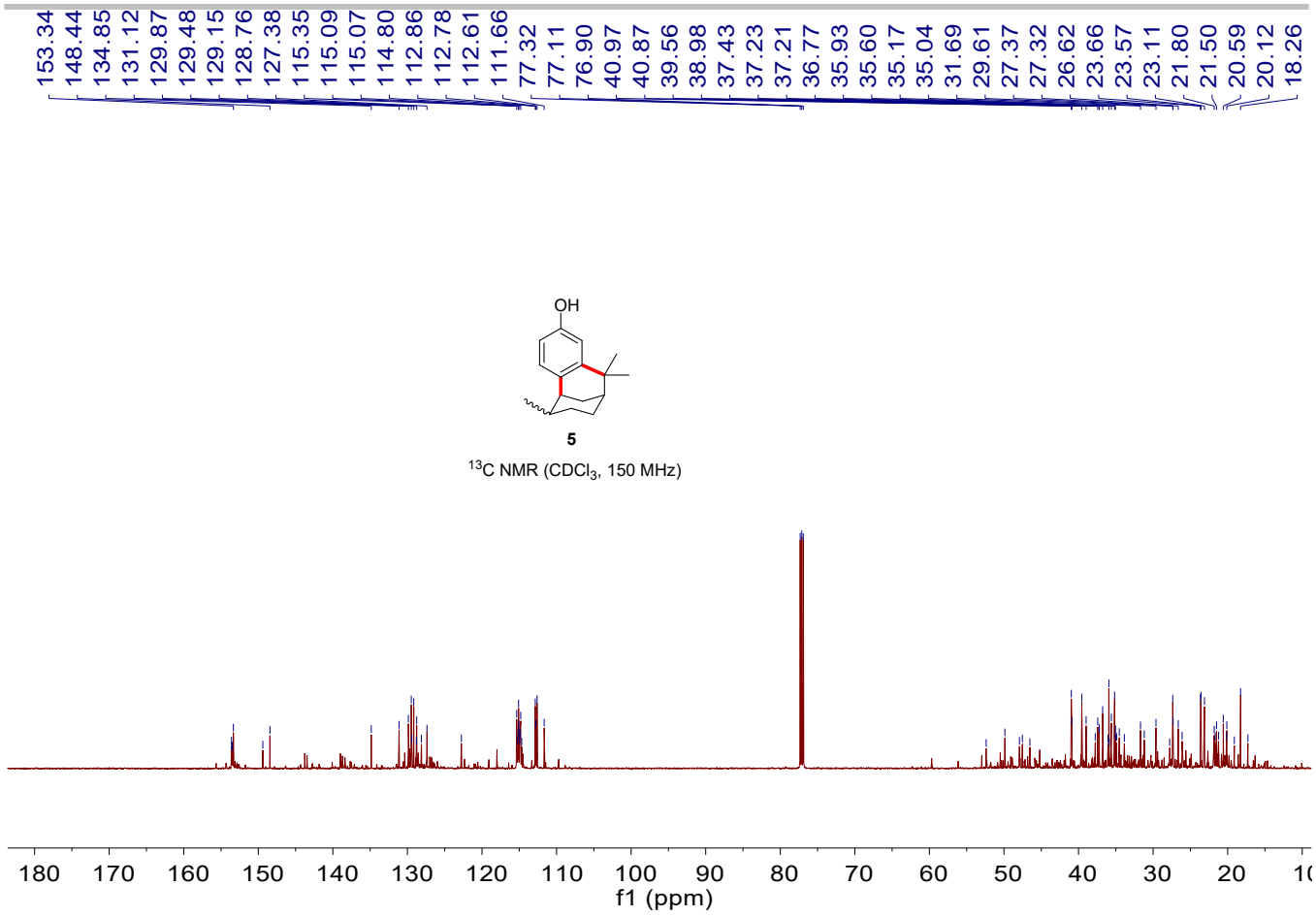

Figure S30. ^{13}C NMR spectrum of product **5**.

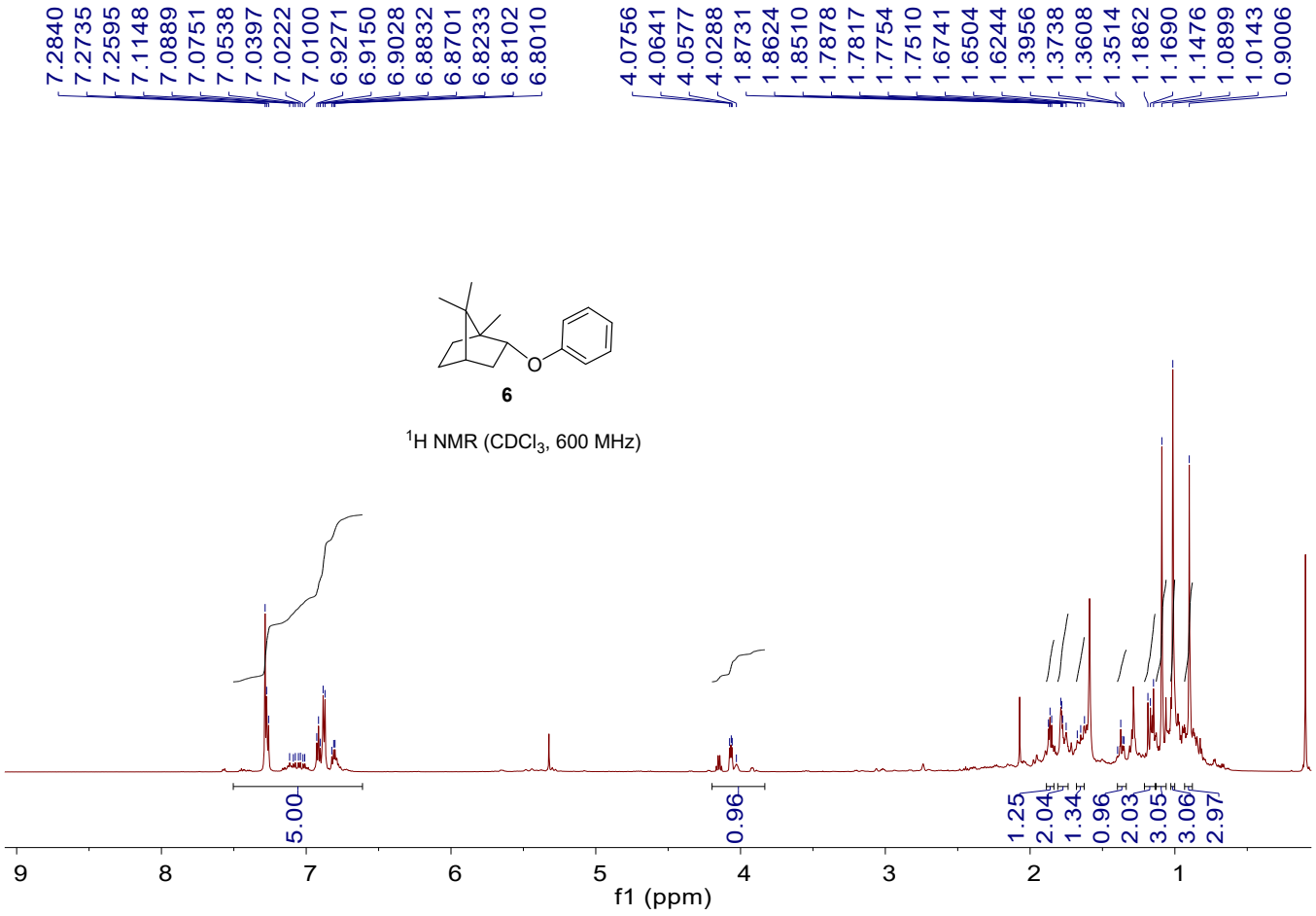

Figure S31. ^{1}H NMR spectrum of product **6**.

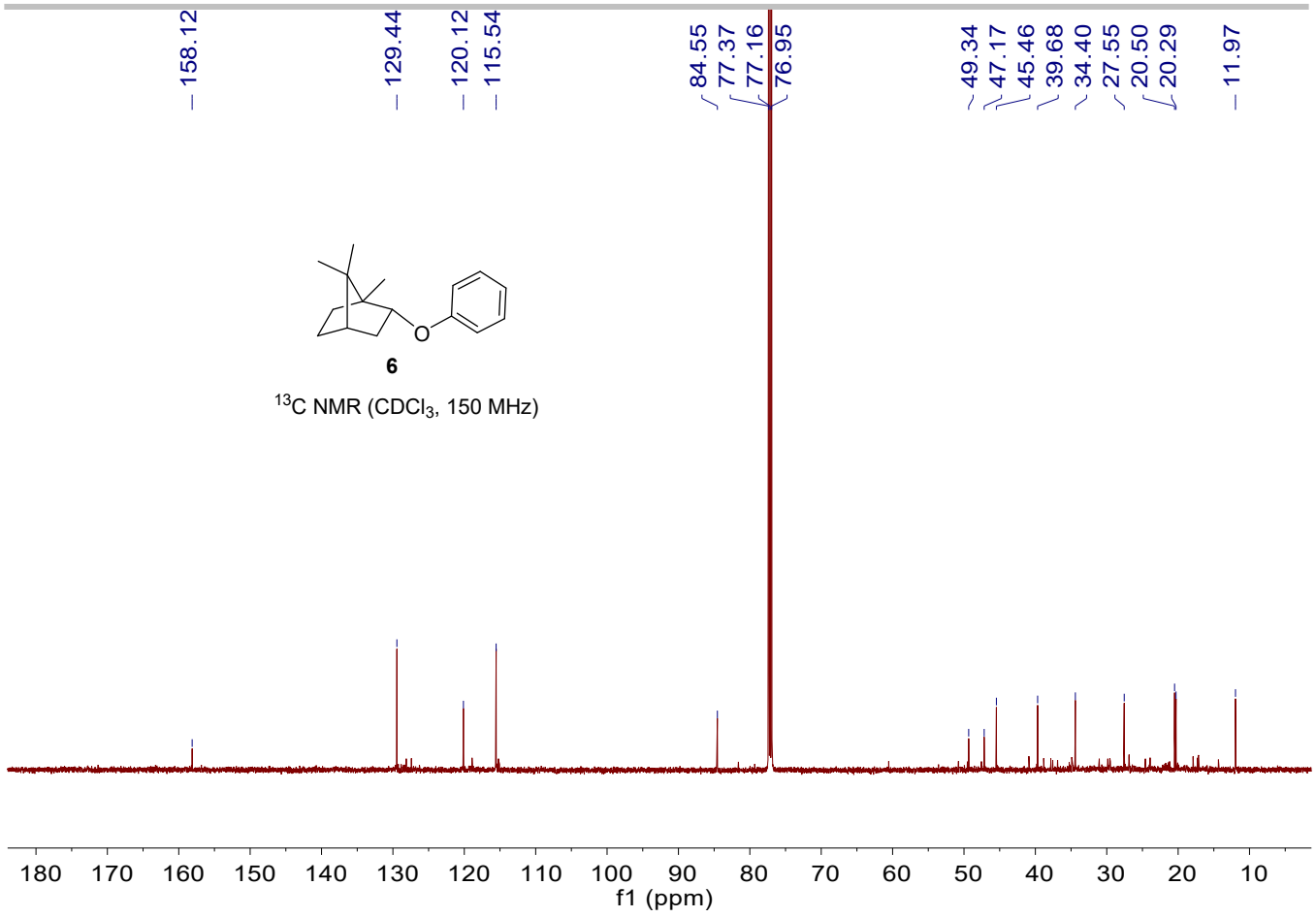

Figure S32. ^{13}C NMR spectrum of product **6**.

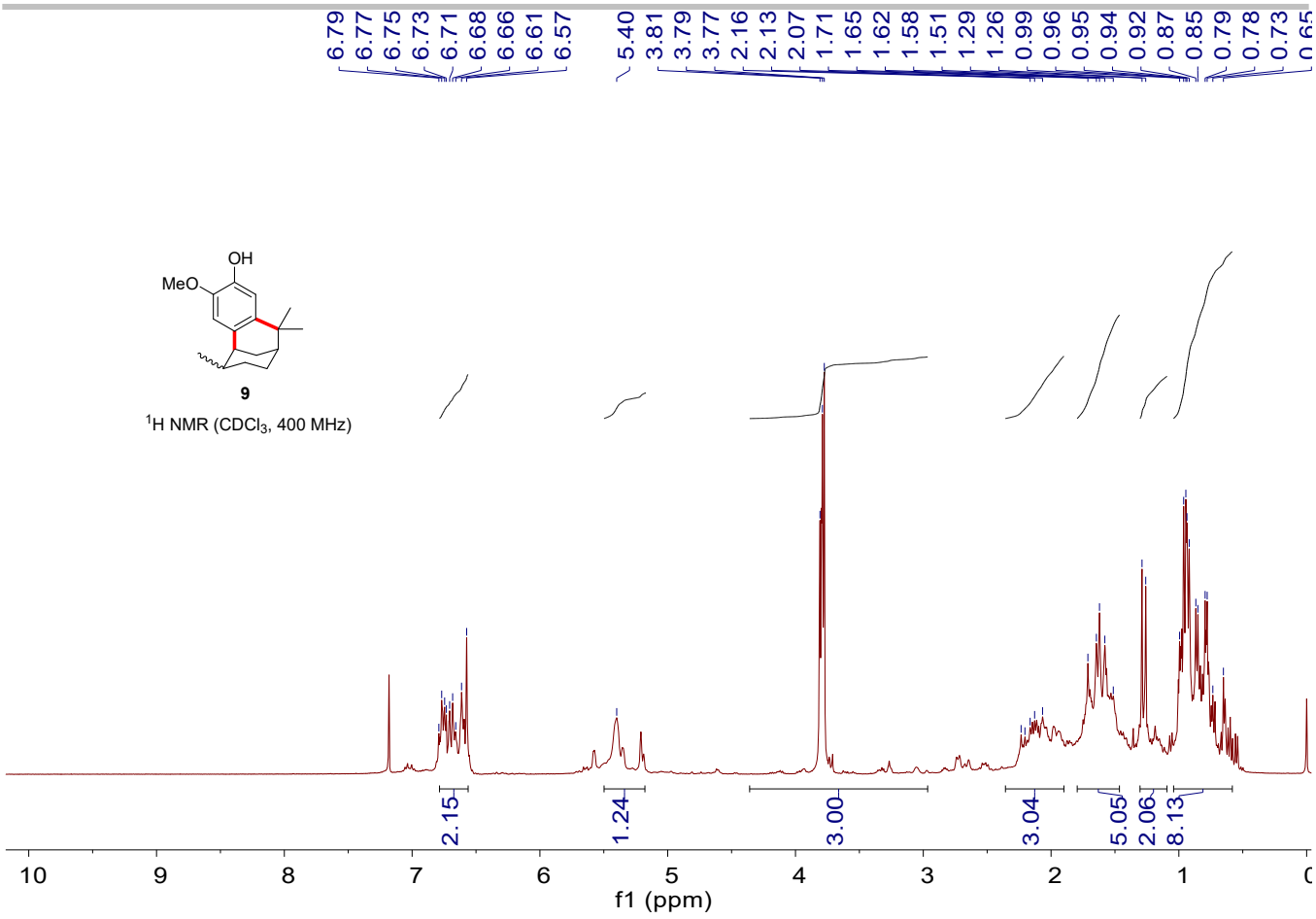

Figure S33. ^{1}H NMR spectrum of product **9**.

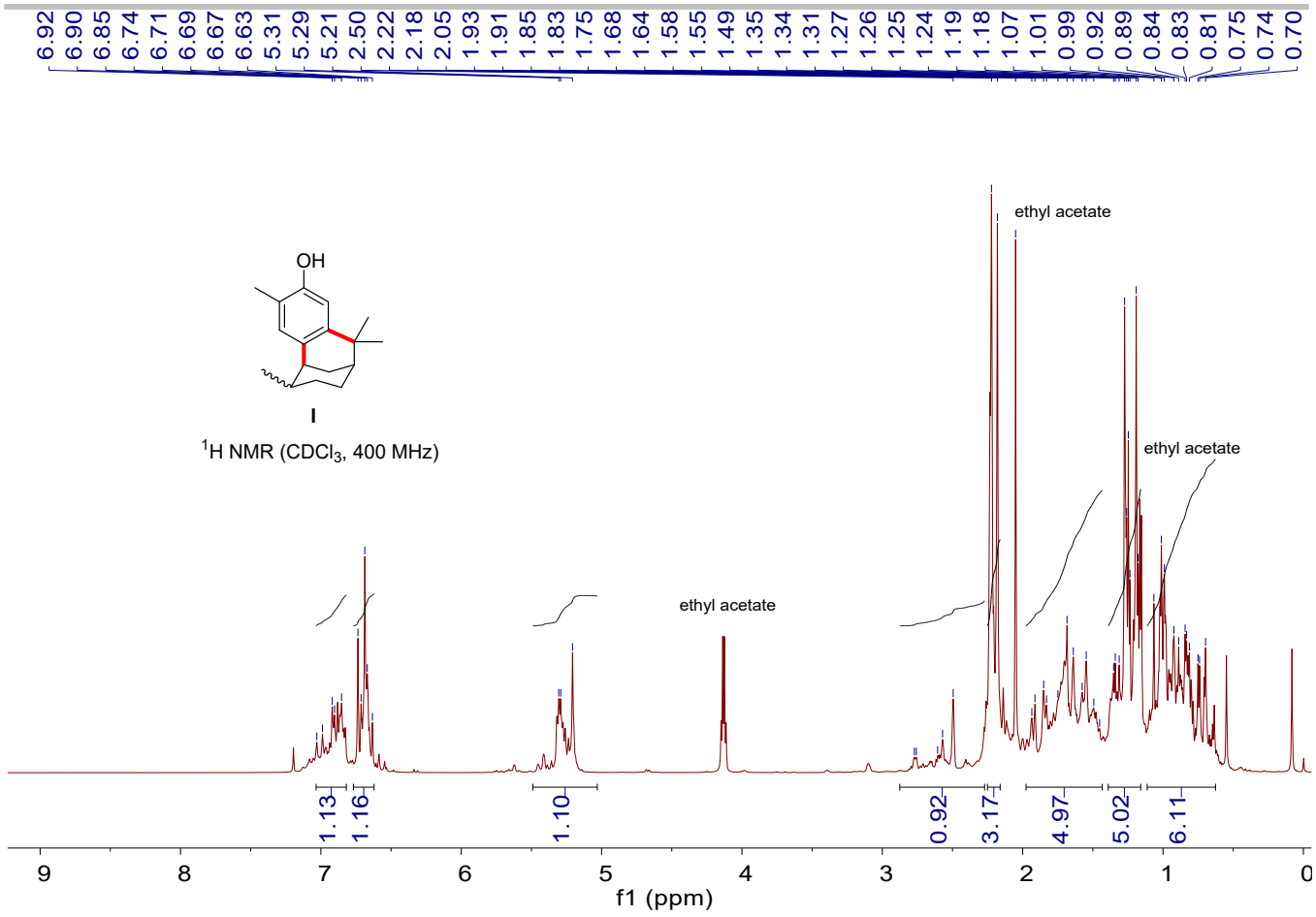

Figure S34. ^{1}H NMR spectrum of product **I**.

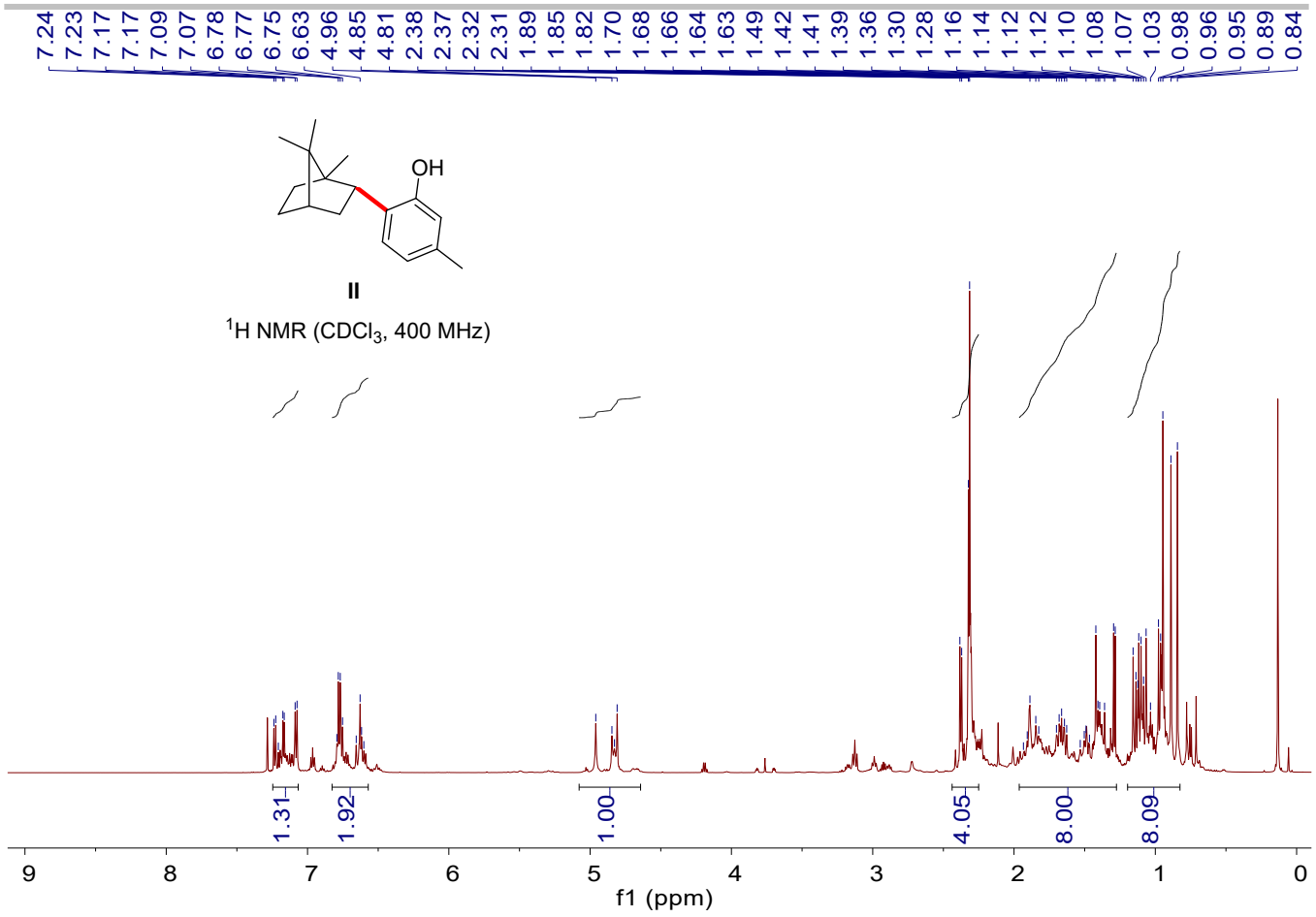

Figure S35. ^{1}H NMR spectrum of product **II**.

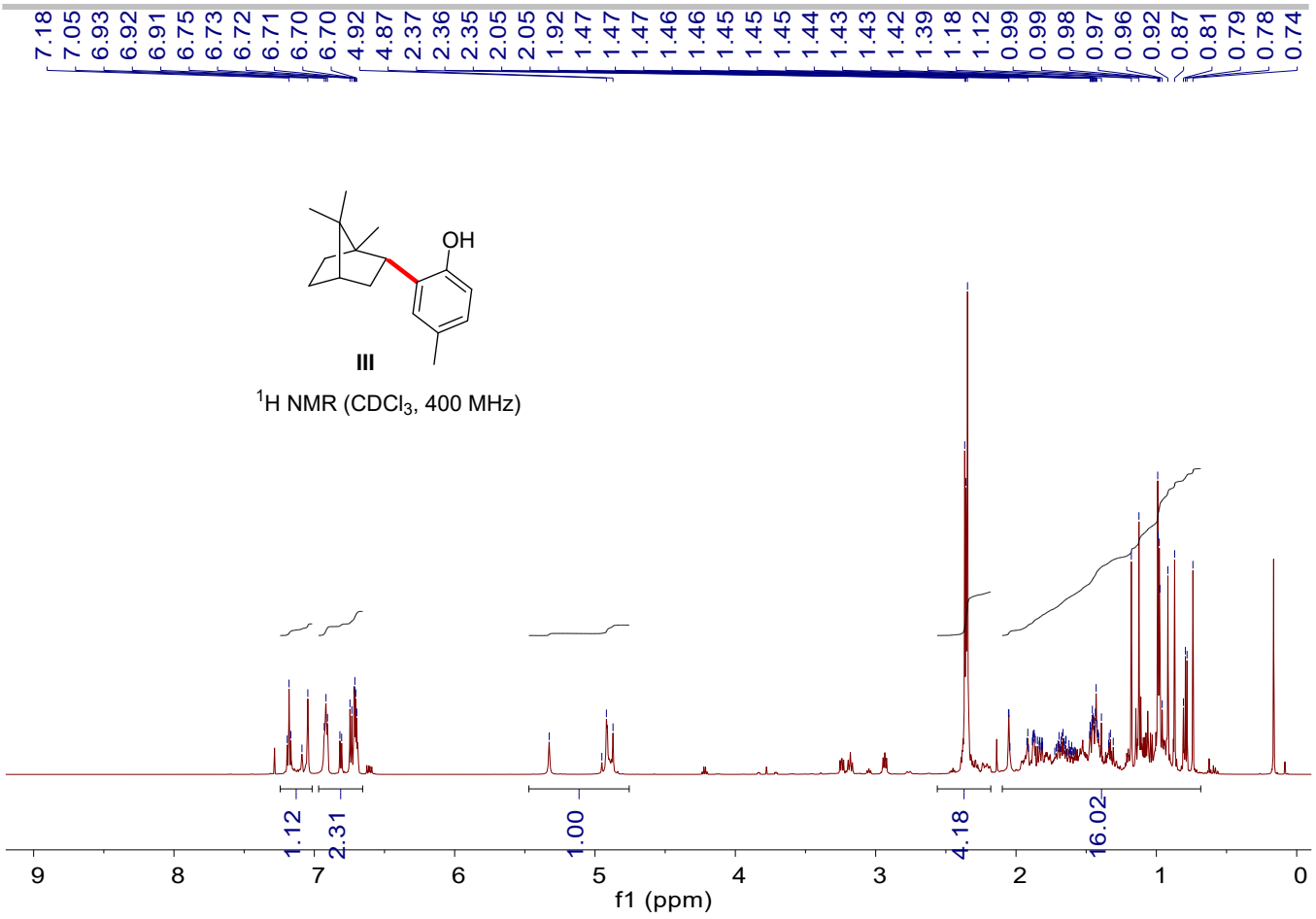

Figure S36. ^{1}H NMR spectrum of product **III**.

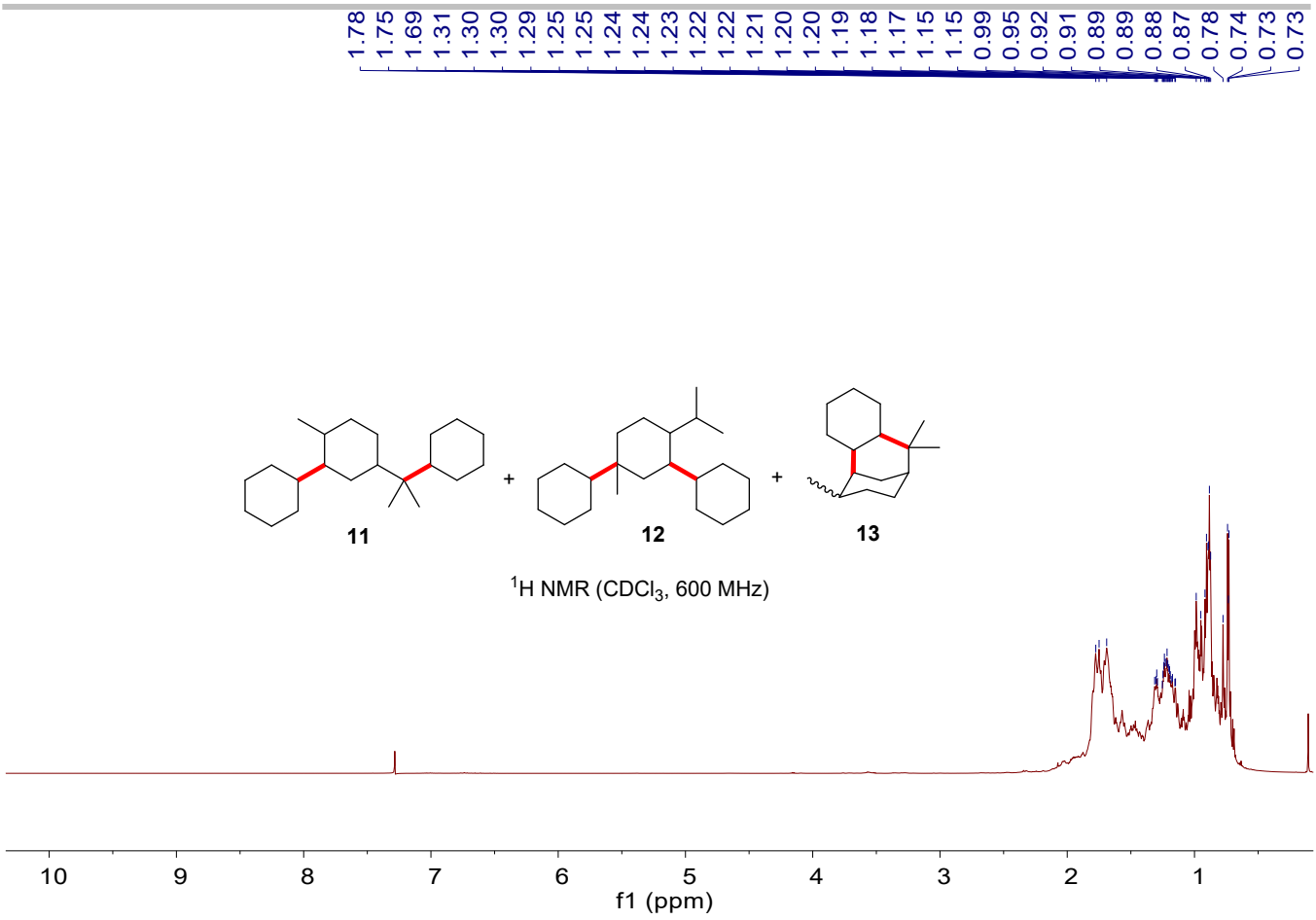

Figure S37. ^{1}H NMR spectrum of products **11-13**.

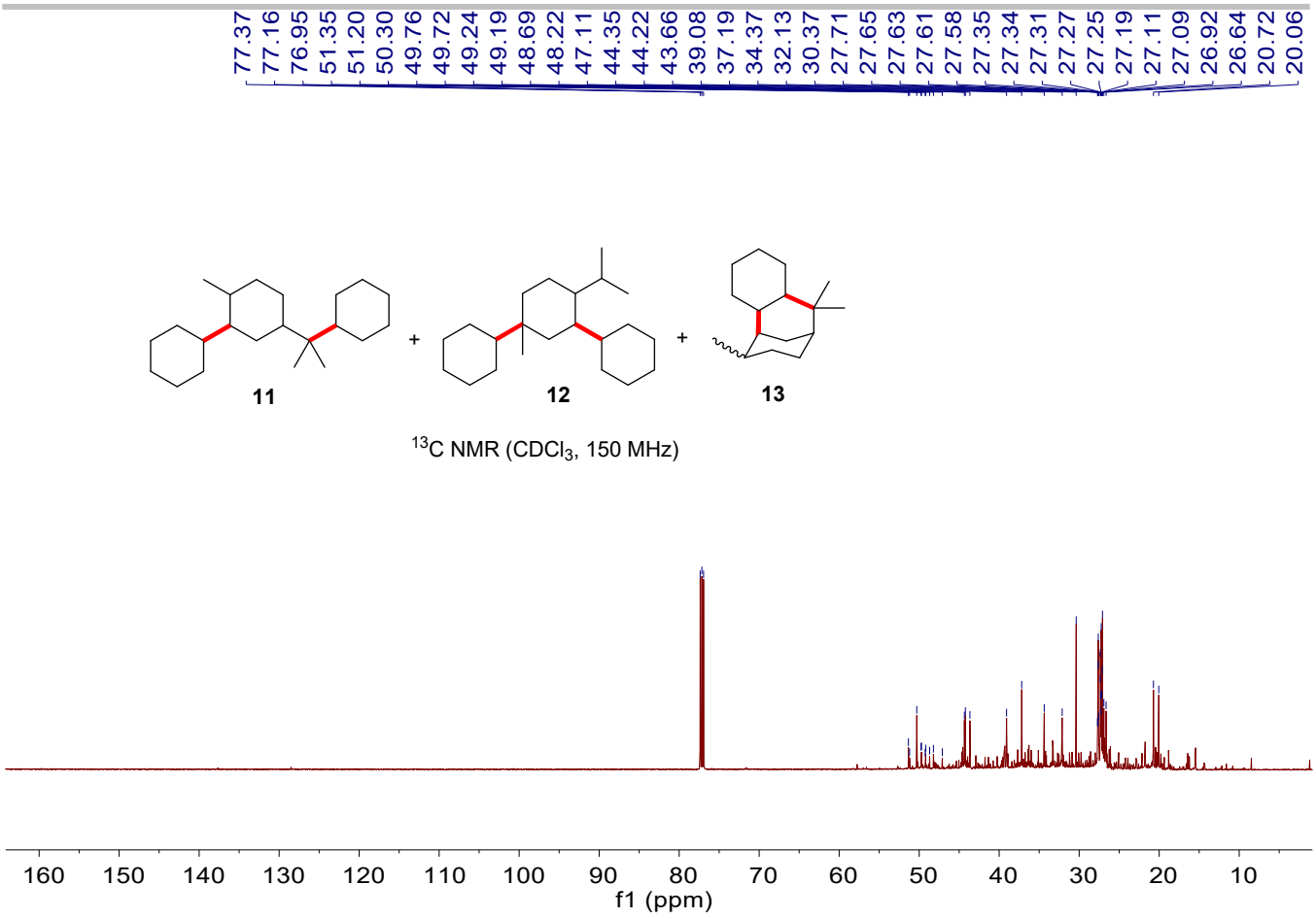

Figure S38. ^{13}C NMR spectrum of products **11-13**.

8. *Catalyst characterization*

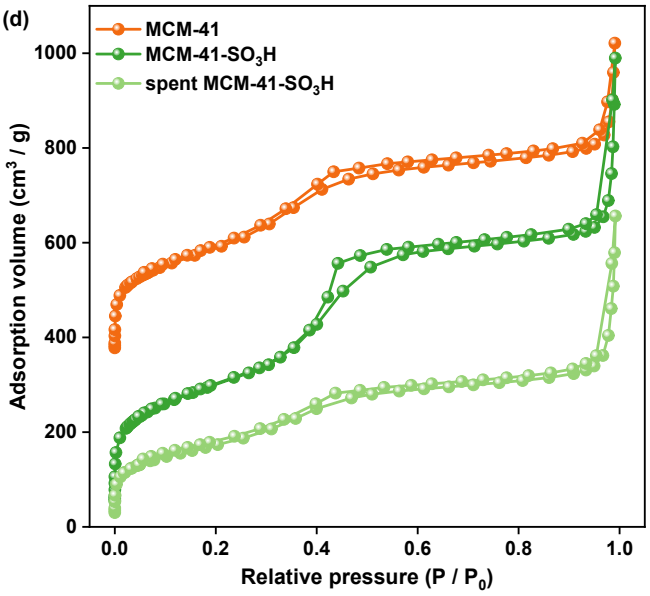

Figure S39. N_2 adsorption-desorption isothermal curves.

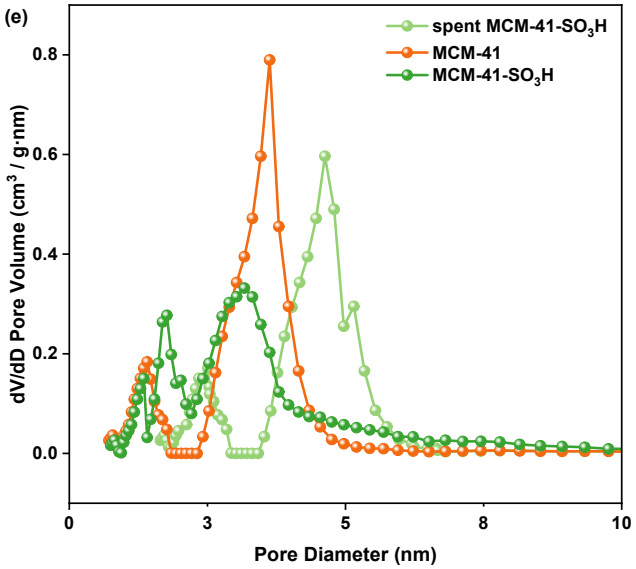

Figure S40. Pore size distribution.

Table S1. Pore characteristics of three catalysts.

Sample	BET surface area ($m^2 \cdot g^{-1}$)	Total pore volume ($cm^3 \cdot g^{-1}$)	Average pore diameter (nm)
MCM-41	891.42	1.45	6.49
MCM-41-SO_3H	801.30	1.02	5.01
spent MCM-41-SO_3H	362.40	0.98	7.18

Table S2. Calculation methodology for various cost categories.

Project	Categories	Method
Capital cost	Equipment cost	Based on actual project consumption
	Other capital cost	57.84% ∝ FCI
Operation cost	Electricity	Based on actual project consumption
	Maintenance	2% of equipment cost
	Labor	10^5 CNY/a/person
	Depreciation	Straight-line method over 20 years
	Other operation cost	Administrative fee + insurance fee = 45% ∝ labor cost + 1% ∝ capital cost